NASA TECHNICAL NOTE

NASA TN D-3739

c.1

NASA TN D-3739

JUPITER HIGH-THRUST ROUND-TRIP TRAJECTORIES

by Roger W. Luidens, Brent A. Miller, and Jay M. Kappraff

Lewis Research Center

Cleveland, Ohio

NATIONAL AERONAUTICS AND SPACE ADMINISTRATION • WASHINGTON, D. C. • DECEMBER 1966

NASA TN D-3739

JUPITER HIGH-THRUST ROUND-TRIP TRAJECTORIES

By Roger W. Luidens, Brent A. Miller, and Jay M. Kappraff

Lewis Research Center
Cleveland, Ohio

NATIONAL AERONAUTICS AND SPACE ADMINISTRATION

For sale by the Clearinghouse for Federal Scientific and Technical Information
Springfield, Virginia 22151 – Price $2.00

JUPITER HIGH-THRUST ROUND-TRIP TRAJECTORIES

by Roger W. Luidens, Brent A. Miller, and Jay M. Kappraff
Lewis Research Center

SUMMARY

The propulsion requirements are analyzed for round trips to Jupiter using the following four concepts to reduce the mission $\sum \Delta V$: (1) optimize the heliocentric transfer angles, (2) use low periapsis elliptical parking orbits at Jupiter, (3) use atmosphere braking at Earth return, and (4) use hyperbolic rendezvous at Jupiter. Total trip times of 500 to 2200 days and stay times of 0 to 200 days were considered. The present study also considers several types of maneuvers for entering and leaving an elliptical parking orbit, a range of elliptical parking orbit apoapses, trajectories lying out of the plane of the ecliptic, and symmetrical (transit times and angles the same for the outbound and the inbound legs) and unsymmetrical trips. The analysis assumes successive two-body trajectories, impulsive thrusting, and circular coplanar planetary orbits. The criterion for comparing the various trajectories is the required total propulsive velocity increment.

With a low circular parking orbit at Jupiter and propulsive braking at Earth return, even the double Hohmann stopover round trip (the trip with the global minimum $\sum \Delta V$) yields a high value for $\sum \Delta V$ (29 miles/sec). The use of atmospheric braking at Earth return and of elliptical parking orbits at Jupiter can markedly reduce the $\sum \Delta V$ required for Jupiter stopover round trips. For example, the minimum total ΔV required for the 1000-day trip with a 100-day stay time can be reduced from 34 to 8 miles per second. This is typical of the ΔV reduction possible for the other trips investigated. The resulting ΔV's are comparable to those for Mars stopover round trips.

Atmospheric braking at Earth allows nonstop trips of 1400 days and longer to be flown for a total ΔV of approximately 4 miles per second. This is about half the ΔV required for the best stopover trip and is comparable to the ΔV for Mars flybys. This difference in ΔV between the stopover and nonstop trips can be used to advantage in the hyperbolic rendezvous mission.

INTRODUCTION

Extensive studies have been made of the possible one-way, nonstop, and stopover

round-trip trajectories to the near planets of Mars and Venus (e.g., refs. 1 to 8). Recently one-way trajectories to Jupiter have been presented in reference 9. Little attention, however, has been given to stopover round-trip trajectories to Jupiter. Some of the reasons for this are related to trajectories. Cursory studies suggest long trip times and high propulsive velocity increments for the Jupiter trip. For example, the double Hohmann stopover round trip to Jupiter has a trip time of 6 years compared with about 3 years for a similar trip to Mars. When a low circular parking orbit at Jupiter and all-propulsive maneuvers are used, the total propulsive velocity increment for the double Hohmann (minimum $\sum \Delta V$) Jupiter round trip is 29 compared with 7 miles per second for Mars, or four times the value for the Mars trip.

Irrespective of the apparent difficulties of the trip, there are several scientific reasons for being interested in the exploration of Jupiter. It is the nearest of the "giant planets" that have characteristics greatly different from the terrestrial planets of Mercury, Venus, and Mars. It has been suggested that Jupiter may have some of the characteristics of a star. Jupiter also has an extensive system of moons that are of interest.

There are several concepts for reducing the mission propulsion requirements from the high values suggested earlier, even for trips of shorter duration than the double Hohmann trip. First, for a given trip duration and stay time, the leg travel angles can be selected to minimize the propulsion requirements. Second, the use of elliptic parking orbits at the target planet, as described in reference 7, is a particularly powerful way to reduce propulsion requirements for trips to the massive planets. Third, atmospheric braking may be used at Earth return. Fourth, several techniques of rendezvous at Jupiter can be used to reduce the propulsive ΔV for part of the mission loads.

This report will examine the previously mentioned concepts and several related ones in an attempt to find trajectories and modes of operation with low propulsion requirements.

The present study considers the following: round-trip durations of 500 to 2200 days (which includes the double Hohmann trip); stay times of 0 to 200 days; several types of Jupiter parking orbits; a range of elliptical parking orbit apoapses; symmetrical and unsymmetrical trips; the effect of atmospheric braking at Earth; rendezvous at Jupiter; and trajectories to avoid the asteroid belt.

METHOD OF ANALYSIS

General Approach

A typical stopover round trip to Jupiter is shown in figure 1. The trip starts from a 1.1 Earth radii circular orbit. A propulsive velocity increment ΔV_1 is impulsively applied in Earth orbit to send the space vehicle toward Jupiter. The heliocentric angle tra-

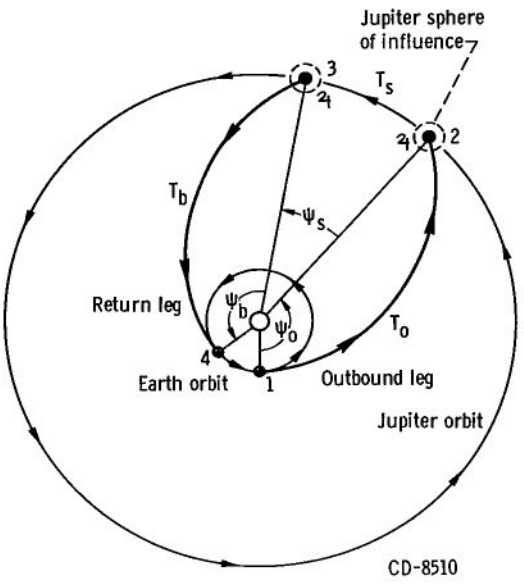

Figure 1. - Typical stopover round-trip trajectory to Jupiter.

versed and the outbound travel time from Earth to Jupiter are ψ_o and T_o, respectively. (The symbols are defined in the appendix.) The outbound travel time and angle are defined from Earth orbit to the periapsis of the trajectory arriving at Jupiter. A second velocity increment ΔV_2 is imparted to the vehicle in the vicinity of the trajectory periapsis at Jupiter to establish a parking orbit about the planet. During the stay time T_s in the parking orbit, both Jupiter and the vehicle traverse the heliocentric angle ψ_s. At the end of the stay, a third propulsive velocity increment ΔV_3 starts the spacecraft on a trajectory back to Earth. The return trajectory covers the heliocentric angle ψ_b and time T_b. At Earth return either propulsive braking to a low circular orbit, ΔV_4, or atmospheric braking, $\Delta V_4 = 0$, is used. (Combinations of atmospheric braking and propulsive braking are not considered.)

The objective of this analysis is to find those trajectories that yield a minimum total propulsive velocity increment $\sum \Delta V$ (where $\sum \Delta V = \Delta V_1 + \Delta V_2 + \Delta V_3 + \Delta V_4$) for a given total trip time T_T and stay time at the destination planet T_s. Several basic relations can be written directly from the description of the mission and figure 1. The total trip time is the sum of the times along the various segments:

$$T_T = T_o + T_s + T_b \tag{1}$$

Also, the heliocentric travel angle of the vehicle ψ_T is the sum of the travel angles along the various segments:

$$\psi_T = \psi_o + \psi_s + \psi_b \tag{2}$$

To achieve a return to Earth, the heliocentric travel angle of the Earth in its orbit about the Sun must be the same as the travel angle of the vehicle about the Sun plus an integral number of revolutions:

$$\psi_\oplus = \psi_o + \psi_s + \psi_b + 360^o N_\oplus \tag{3}$$

If the travel time T_o and the travel angle from Earth to Jupiter periapsis ψ_o (or what

is equivalent, the launch date and travel time) of a trajectory are specified, the transfer orbit elements may be calculated, and hence the terminal heliocentric velocities and path angles may be calculated, by the method of reference 1. In this reference the planetary motions as given by an ephemeris are approximated by mutually inclined ellipses, and the planetary velocity vectors and positions are calculated from these. The interplanetary trajectory of the vehicle is assumed to be composed of planet- and Sun-centered conic segments matched at the sphere of influence. A typical trajectory calculation is made as follows:

(1) A launch date is specified. This defines the position and motion of the Earth when the space vehicle departs from Earth.

(2) An Earth to Jupiter transfer time T_o is selected. This, together with the launch date, defines the position and motion of Jupiter at the arrival of the space vehicle. Together steps 1 and 2 define T_o and ψ_o.

(3) The unique transfer trajectory, three conic sections "patched" together, that connects Earth and Jupiter in the specified outbound leg time is found by an iteration process.

A return leg trajectory may be calculated similarly, where the Jupiter departure date is determined by the arrival date plus the stay time; also, the return leg time is determined by the total trip time and the outbound leg plus stay time.

Interplanetary Trajectories

Jupiter trajectories are considered here at two levels of precision. The more precise technique assumes Jupiter and Earth are in inclined elliptic orbits, as in reference 1 and as mentioned previously. A less precise analysis, wherein Earth and Jupiter are assumed to travel in circular coplanar orbits about the Sun, is used to make a broad survey of many possible trajectories to find those of most interest. These are good approximations as may be seen by examining the eccentricities of the orbits of Earth and Jupiter in table I, where zero eccentricity corresponds to a circular orbit. Consistent with the circular orbit assumption, the angular velocity of the Earth and Jupiter are as-

TABLE I. - PLANETARY CONSTANTS

	Earth	Jupiter
Planet mass, lb	13.2×10^{24}	4200×10^{24}
Planet radius, R, miles	3963	43 410
Gravitational force constant, μ, miles^3/sec^2	9.60×10^{4}	3.06×10^{7}
Average angular velocity about Sun, ω, deg/day	0.986	0.083
Average distance from Sun, AU	1	5.20
Eccentricity of heliocentric orbit	0.01674	0.04837
Inclination to ecliptic, deg	0	1.307
Sphere of influence radius, miles	5.75×10^{5}	3.0×10^{7}

sumed to be equal to their mean angular velocities, also shown in table I. With this assumption,

$$\psi_s = \omega_{\mathcal{A}} T_s \tag{4}$$

and

$$\psi_{\oplus} = \omega_{\oplus} T_T \tag{5}$$

It will be shown later that the minimum $\sum \Delta V$ round-trip trajectories are symmetrical; that is, $T_o = T_b$ and $\psi_o = \psi_b$. For coplanar circular planetary orbits and symmetrical trips, the equations for the total trip time and total travel angle may be written as functions of the two independent variables T_o and ψ_o. Thus, equation (1) becomes

$$T_T = 2T_o + T_s \tag{6}$$

and from equations (3) to (6),

$$T_s = \frac{1}{\omega_{\oplus} - \omega_{\mathcal{A}}} \left(2\psi_o - 2T_o\omega_{\oplus} + 360^{\circ} N_{\oplus}\right) \tag{7}$$

When the numerical values for the orbital characteristics of Earth and Jupiter listed in table I are used, equation (7) may be written as

$$T_s = 2.21\,\psi_o - 2.18\,T_o + 398.0\,N_{\oplus} \tag{8}$$

Further consequences of assuming a symmetrical trip are that $\Delta V_1 = \Delta V_4$, $\Delta V_2 = \Delta V_3$, and $\Delta V_1 + \Delta V_2 = \Delta V_3 + \Delta V_4$. Also, a minimum $\sum_1^4 \Delta V$ round trip now consists of two legs, each of which corresponds to a minimum $\Delta V_1 + \Delta V_2$ leg.

Minimum $\Delta V_1 + \Delta V_2$ legs. - To find those interplanetary legs that yield a minimum $\Delta V_1 + \Delta V_2$, a reference parking orbit at Jupiter is selected. The reference parking orbit is a circular one at 1.1 Jupiter radii. For the reference parking orbit, the ΔV may be calculated as described in the later section on parking orbits.

Minimum $\Delta V_1 + \Delta V_2$ legs for specified outbound leg times T_o are found by searching over a range of Earth departure dates (or what is equivalent, a range of travel angles ψ_o). Typical results for T_o = 215, 544, and 1088 days are shown in figure 2(a), (b), and (c), respectively. Several general observations may be made about these data:

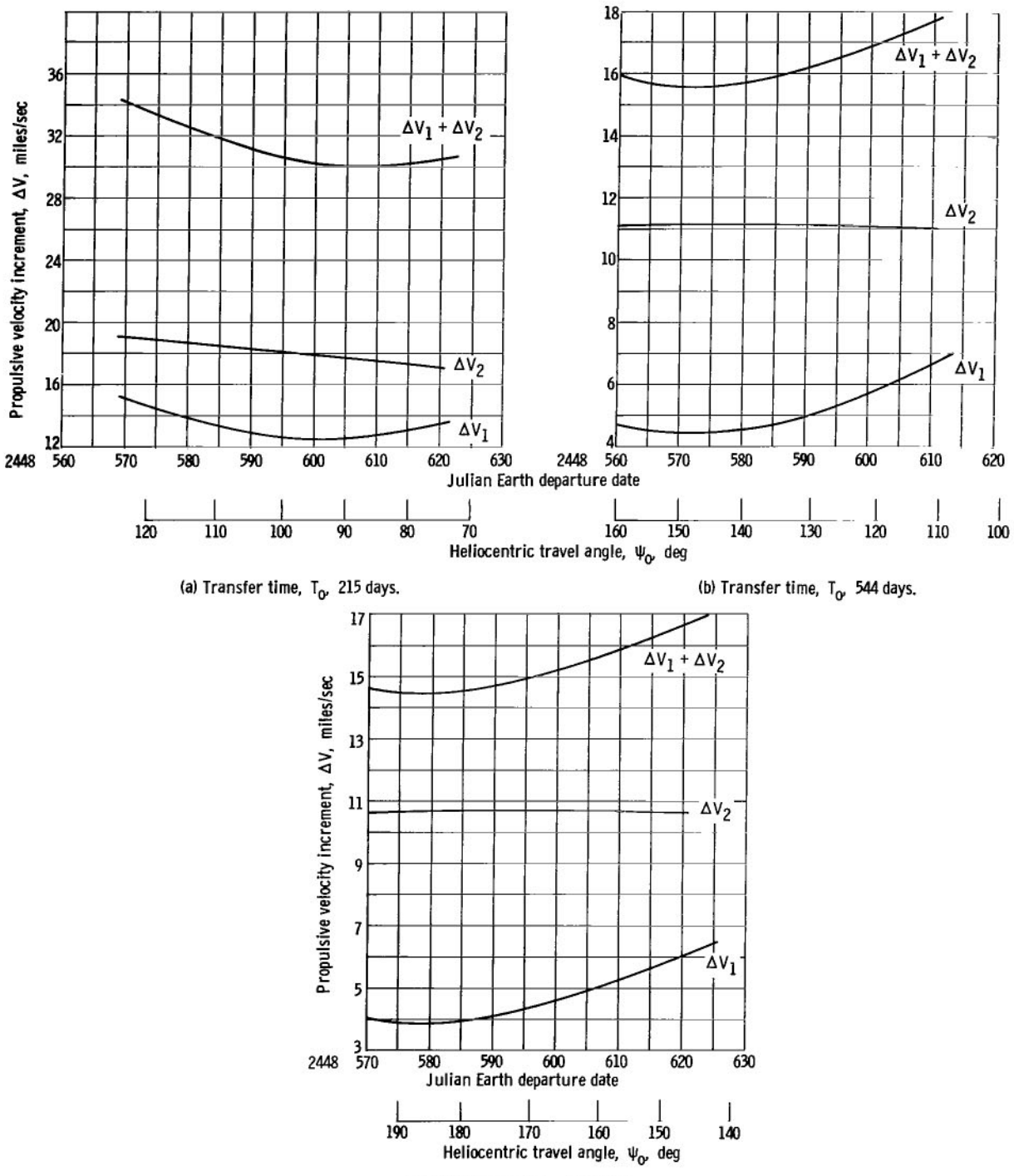

Figure 2. - Variation of propulsive velocity increments for Earth to Jupiter transfer with Earth departure date and heliocentric travel angle.

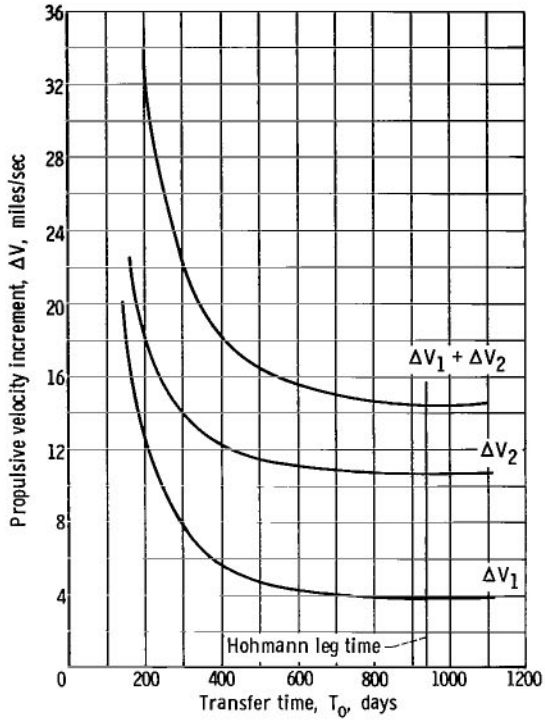

Figure 3. - Variation of Earth departure and Jupiter arrival propulsive velocity increments with transfer time for minimum $(\Delta V_1 + \Delta V_2)$ trajectories.

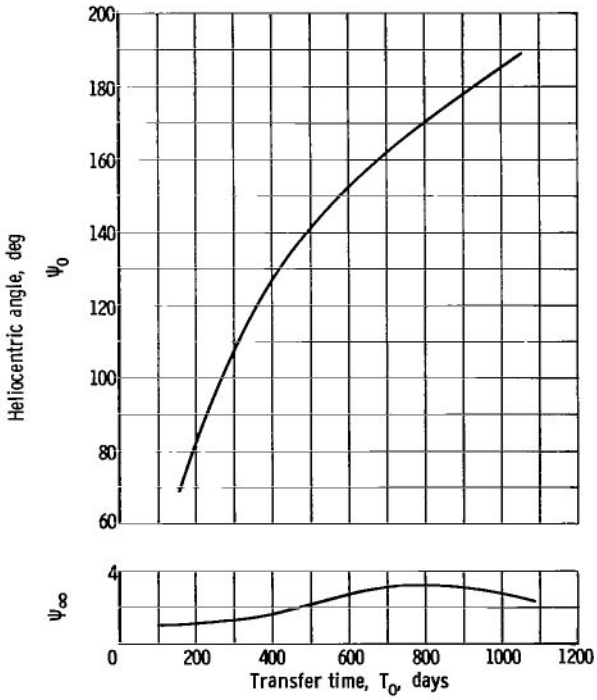

Figure 4. - Variation of Earth to Jupiter travel angle ψ_o and ψ_∞ with transfer time for minimum $(\Delta V_1 + \Delta V_2)$ trajectories.

(1) The departure date for minimum $\Delta V_1 + \Delta V_2$ is near that for minimum ΔV_1 (the ΔV to leave Earth).

(2) There is little difference, about 6 days, in the departure date for minimum $\Delta V_1 + \Delta V_2$ for T_o from 544 to 1088 days. Because the best Earth departure date varies only slightly with outbound leg time, longer leg times result in a corresponding delay in Jupiter arrival date.

The minimum $\Delta V_1 + \Delta V_2$ from curves like these and the corresponding individual values of ΔV_1 and ΔV_2 are plotted against their outbound leg time in figure 3. The $\Delta V_1 + \Delta V_2$ curve has a monotonically decreasing slope up to the one-way Hohmann leg time of about 940 days. Because of the monotonically decreasing slope of this curve (the curve for the return leg is the same), it can be deduced that for a given total trip duration and all propulsive maneuvers (i. e., no atmospheric braking) the symmetrical trajectories give the lowest $\sum \Delta V$. This point is illustrated later.

Total trip time and stay time. - The transfer angles ψ_o corresponding to the minimum $\Delta V_1 + \Delta V_2$ legs also result from the method of reference 1 and are plotted in figure 4 as a function of the mission duration. With these values of ψ_o, the total trip and stay times for the minimum $\sum \Delta V$ symmetric trajectories may be calculated from equations (6) and (7). The results are shown in figures 5 and 6 for stay times less than a synodic period (about 1 yr). The integral number of revolutions of Earth about the Sun $N_\oplus$ are noted for the various trips on the curves. The total trip times for minimum $\sum \Delta V$ trips (fig. 5) occur in very

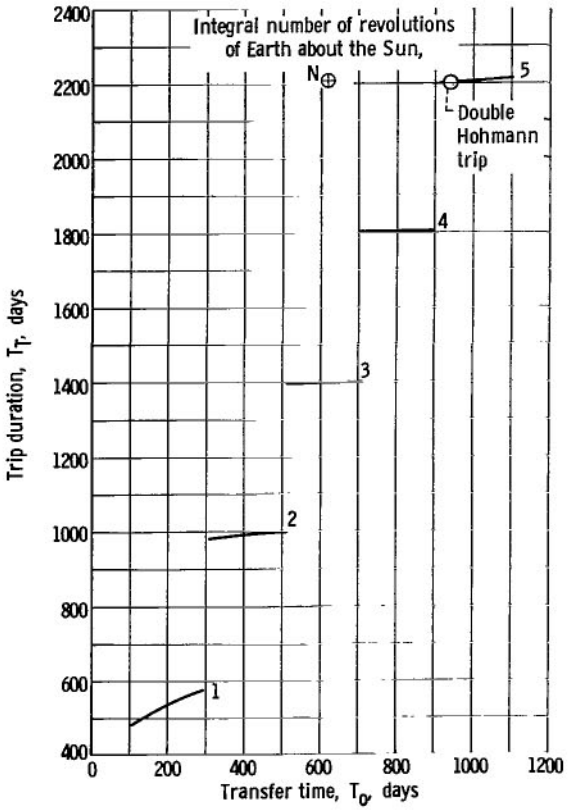

Figure 5. - Variation of mission duration with Earth to Jupiter transfer time for minimum ($\Delta V_1 + \Delta V_2$) symmetrical trajectories.

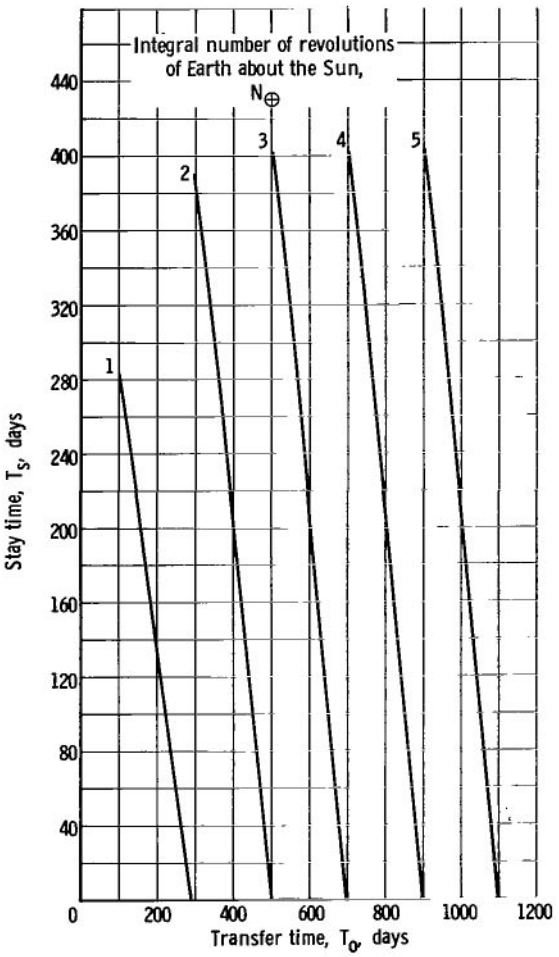

Figure 6. - Variation of Jupiter stay time with Earth to Jupiter transfer time for minimum ($\Delta V_1 + \Delta V_2$) symmetrical trajectories.

narrow bands of trip duration corresponding to discrete values of $N_\oplus$. The double Hohmann trip is indicated by the circle symbol.

The stay time (fig. 6) varies almost linearly with leg time T_o. The slopes of the lines are such that an increase of 1 day in the T_o decreases the stay time about 2 days. This results because increasing T_o 1 day also increases the T_b 1 day (from symmetry), and because the Earth departure and arrival dates stay nearly constant as was observed earlier.

Procedure for calculating round trips. - The characteristics of trips with a specified stay time may be calculated as follows using the information presented thus far:

(1) Select an available total trip time from figure 5 and note the value of $N_\oplus$.

(2) With the previous value of $N_\oplus$ read the T_o for the specified stay time from figure 6.

(3) The values of ΔV are then given in figure 3 as a function of T_o. For an all-propulsive trip,

$$\sum \Delta V = 2(\Delta V_1 + \Delta V_2)$$

For a trip using full atmospheric braking at Earth return,

$$\sum \Delta V = (\Delta V_1 + \Delta V_2) + \Delta V_2$$

Sphere of Influence to Periplanet

The preceding discussion was based on knowing T_o, ψ_o, T_b, ψ_b, and T_s. The method of reference 1 describes how the values of T_o and ψ_o are obtained for one leg of a round trip. This section describes how the information for two single legs is combined to yield a round trip, and also prepares the way for the following section dealing with parking orbits by describing the trajectories inside the Jupiter sphere of influence in detail. The matching of the inbound and outbound legs occurs in the vicinity of Jupiter and is part of the parking orbit arrival or departure maneuver.

Planetocentric coordinates. - It is convenient to describe the trajectory in the vicinity of Jupiter, that is, within the Jupiter sphere of influence, in coordinates centered on the planet. An appropriate coordinate system is shown in figure 7(a); the x-axis is the Jupiter-Sun line, with the positive x-axis directed away from the Sun, and the y-axis forms a right-hand system when viewed from the north ecliptic pole. The x-direction is set at the time of arrival of the vehicle at the Jupiter sphere of influence and is thereafter fixed in inertial space; that is, while the center of the coordinate system moves with Jupiter, the x-axis continues to point at a fixed point on the celestial sphere.

The change from heliocentric to planetocentric coordinates is made at the sphere of influence - a sphere of radius $r_\infty \approx 3\times10^7$ miles about Jupiter, shown schematically in figure 7(a), and to scale in figure 1 (p. 3). The change is made by taking the vector difference between the vehicle heliocentric velocity vector V_H and the planet velocity vector $V_{\mathcal{J}}$, both at the time of arrival at the sphere of influence. This gives the planetocentric hyperbolic excess velocity vector defined by V_∞ and α_∞, where α_∞ is measured with respect to the local heliocentric horizontal at the time of arrival at the sphere of influence. Using the law of cosines gives

$$V_\infty = \left[V_H^2 + V_{\mathcal{J}}^2 - 2V_H V_{\mathcal{J}} \cos(\alpha_H - \psi_\infty)\right]^{1/2} \tag{9}$$

and

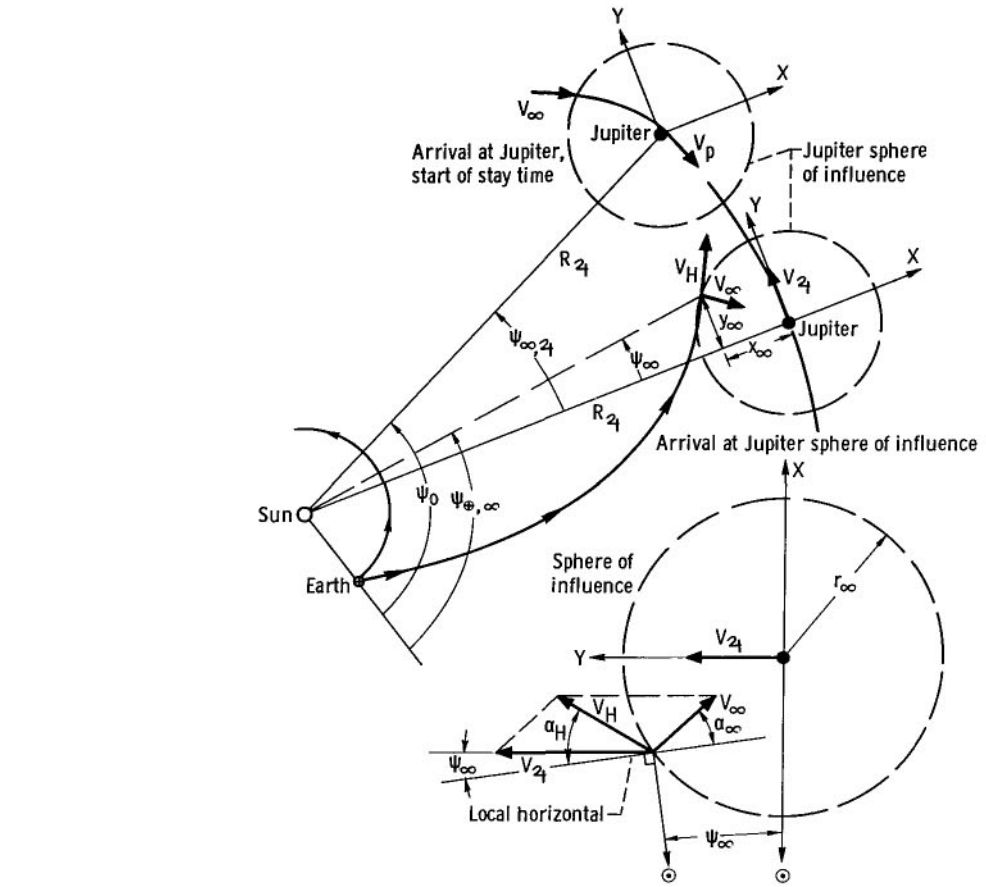

(a) Change from heliocentric to planetocentric coordinates.

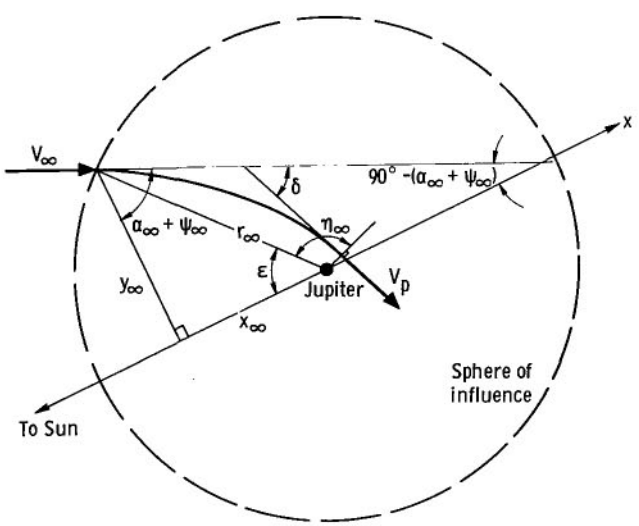

(b) Planetocentric trajectory within sphere of influence in planetocentric coordinates.

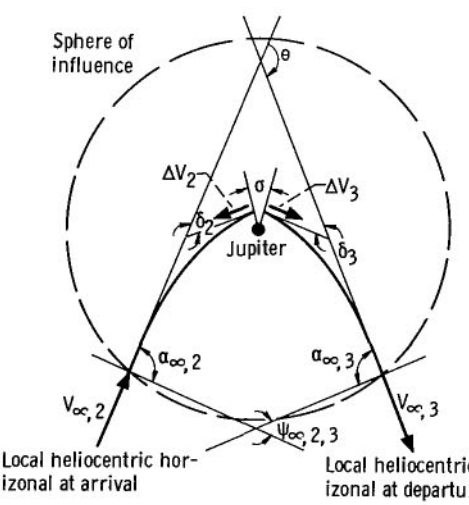

(c) Conditions for a round trip in planetocentric coordinates.

CD-8511

Figure 7. - Geometry of trajectories in the vicinity of Jupiter.

$$\alpha_\infty = \cos^{-1}\left(\frac{V_\infty^2 + V_{2}^2 - V_H^2}{2V_\infty V_{2}}\right) - \psi_\infty \tag{10}$$

The vector V_∞ is located at (x_∞, y_∞) on the sphere of influence.

Times and angles. - The outbound heliocentric angle ψ_o is determined by the angles shown in figure 7(a):

$$\psi_o = \psi_{\oplus,\infty} + \psi_{\infty,2} - \psi_\infty \tag{11}$$

where $\psi_{\infty,2}$, the heliocentric angle traversed by the planet during the passage in the hyperbolic trajectory from the sphere of influence to the periplanet, is given by

$$\psi_{\infty,2} = \omega_2 T_\infty \tag{12}$$

Also from figure 7(a),

$$\psi_\infty = \arctan\frac{y_\infty}{R_2 + x_\infty} \tag{13}$$

The terms T_∞ and (x_∞, y_∞) remain to be determined.

Inside the sphere of influence and in the x, y-coordinate system, the vehicle trajectory is assumed to be independent of the presence or absence and therefore the position of the Sun. The vehicle has the velocity V_∞ at the sphere of influence, which is at a great distance from the planet (figs. 7(b) and (c)), and approaches Jupiter along a hyperbolic trajectory, which passes through a periapsis of radius r_p with the velocity V_p.

The eccentricity of the approach hyperbola is

$$e = \frac{V_\infty^2 r_p}{\mu_2} + 1 \tag{14}$$

and the semilatus rectum is

$$p = r_p(1 - e) \tag{15}$$

In terms of the previous two parameters, the time to travel from the sphere of influence to the planet on the approach hyperbola is

$$T_\infty = \frac{1}{e^2 - 1}\sqrt{\frac{p}{\mu}}\left[\frac{ep \sin \eta_\infty}{1 + e \cos \eta_\infty} - \frac{p}{\sqrt{e^2 - 1}} \ln\left(\frac{e \sin \eta_\infty + \sqrt{e^2 - 1}}{1 + e \cos \eta_\infty} + \frac{1}{\sqrt{e^2 - 1}}\right)\right] \tag{16}$$

where η_∞ is the true anomaly of the vehicle at the sphere of influence, which is given by

$$\eta_\infty = \cos^{-1}\left[\frac{1}{e}\left(\frac{p}{r_\infty} - 1\right)\right] \tag{17}$$

The position of V_∞ on the sphere of influence (x_∞, y_∞), which is also specified by (r_∞, ϵ), may be found in terms of α_∞ by the following relation from the geometry of figure 7(b):

$$\epsilon = 180^\circ - \eta_\infty - \alpha_\infty - \psi_\infty + \delta \tag{18a}$$

where

$$\tan \epsilon = \frac{y_\infty}{x_\infty} \tag{18b}$$

The terms η_∞, α_∞, and ψ_∞ are given by equations (17), (10), and (13), respectively. The turning due to gravity is δ_i, and for a sphere of influence large compared with the periapsis radius, which is generally the case, it is given to a good approximation by

$$\delta_i = \sin^{-1}\frac{1}{\overline{V}_\infty^2 + 1} \tag{19a}$$

where

$$\overline{V}_\infty^2 = \frac{V_\infty^2 r_p}{\mu} \tag{19b}$$

The preceding relations for the trajectory from the sphere of influence to the periplanet are incorporated in the method of reference 1. An iterative procedure is used to find the perigee to peri-Jupiter interplanetary trajectory and the patch point (x_∞, y_∞). The iteration is begun by a massless point to point calculation that neglects the sphere of influence ($\psi_\infty = 0$ in eq. (18a)). A similar analysis applies for the inbound trajectory. When symmetrical inbound and outbound trajectories are assumed, the magnitudes of corresponding trajectory angles and times are the same; for example,

$$\delta_2 = \delta_3$$

$$\psi_{\infty, 2} = \psi_{\infty, 3}$$

and

$$T_{\infty, 2} = T_{\infty, 3}$$

Values of T_∞ and V_∞ are presented in figures 8 and 9, respectively, and values of ψ_∞, which is always less than about 3^o, are presented in figure 4 (p. 7). For comparison, Jupiter traverses a central angle of 1.2^o to 7.3^o while the vehicle is within the Jupiter sphere of influence. These angles are large enough to have a significant effect on the geometry of the trajectories about Jupiter. The time in the sphere of influence (fig. 8) is quite large; it varies from 15 to 88 days, which is significant compared with leg times of between 200 and 1000 days. Thus, in the analysis of Jupiter trajectories it is necessary to account for ψ_∞ and T_∞ to achieve good accuracy. For trajectories to the planets of smaller mass like Mars and Mercury, and even Earth and Venus, the terms

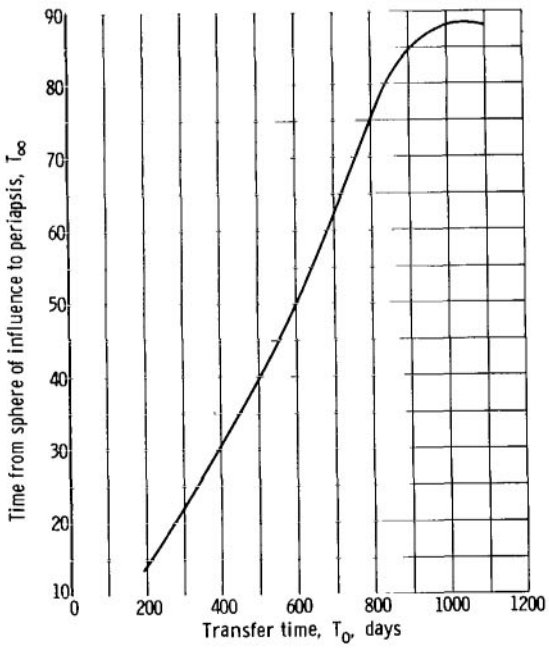

Figure 8. - Variation of time from Jupiter sphere of influence to periapsis of parking orbit with transfer time for minimum ($\Delta V_1 + \Delta V_2$) trajectories.

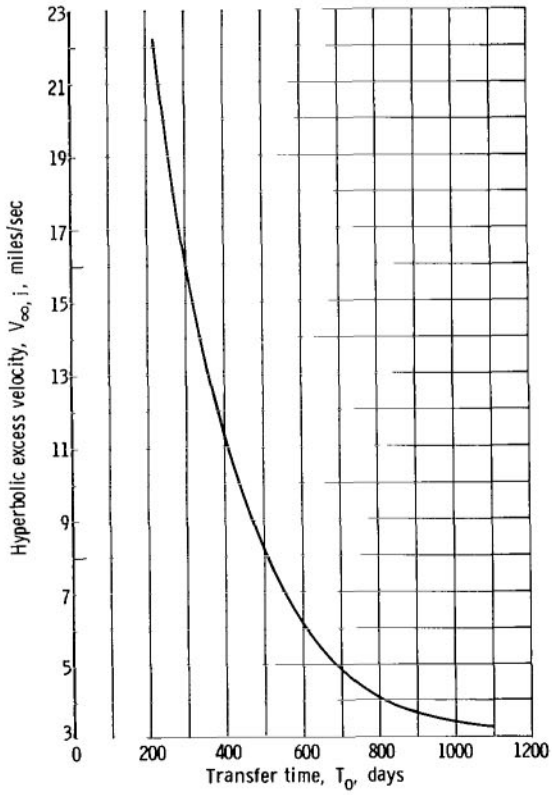

Figure 9. - Variation of hyperbolic excess velocity at Jupiter with transfer time for minimum ($\Delta V_1 + \Delta V_2$) trajectories.

ψ_∞ and T_∞ are both comparatively small. At Earth, for instance, T_∞ is several days, and, to a good approximation, can be neglected.

Angle matching for round trips. - Figure 7(c) shows a view of the approach and departure trajectories within the sphere of influence and in an inertial coordinate system fixed on Jupiter, like the one described previously. To perform a round trip, the vehicle velocity vector at arrival at the sphere of influence of Jupiter must be turned through the angle θ by the time the vehicle reaches the sphere of influence at departure. From the geometry of figure 7(c), and recalling that the trajectories are symmetrical, the required turning θ is

$$\theta = 2\alpha_{\infty,2} - \psi_{\infty,2,3} \tag{20}$$

where $\alpha_{\infty,2}$ is given by equation (10), and $\psi_{\infty,2,3}$, the rotation of the local horizontal during the time the vehicle is within the sphere of influence, is given by

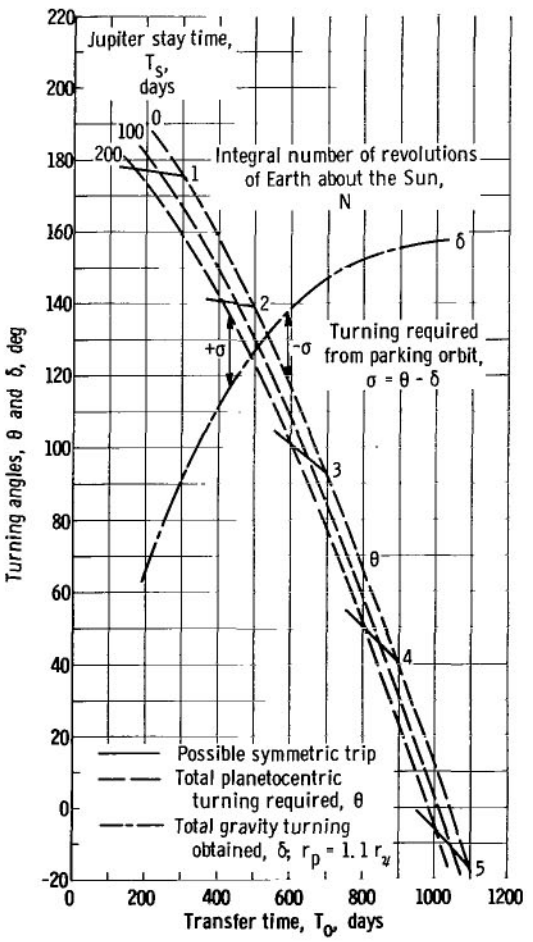

Figure 10. - Variation of total required turning and gravity turning obtained with transfer time.

$$\psi_{\infty,2,3} = \omega_{\mathcal{J}}(T_S + 2T_\infty) - 2\psi_\infty \tag{21}$$

The values of θ for minimum $\Delta V_1 + \Delta V_2$ trips are given in figure 10 as functions of outbound leg time for several stay times. The angle θ increases from a value of near 10° for times near the Hohmann leg time of 940 days to near 180° at a leg time of 200 days.

Parking Orbits

The preceding discussions have defined the boundary conditions that the trajectories within the sphere of influence must meet to complete a round trip, namely, $V_{\infty,2}$ and $V_{\infty,3}$ of figure 9 and θ of figure 10. In this section the maneuvers and parking orbits that satisfy these boundary conditions are discussed. A detailed analysis of the various kinds of parking orbits is given in reference 7. Only a brief review of the parking orbits is given here. The further assump-

tions made for the parking orbit analyses are as follows:

(1) The planet is spherically symmetric (nonoblate).

(2) The maneuvers are made impulsively.

(3) The minimum periapsis consistent with avoiding atmosphere effects is somewhat arbitrarily taken as 1.1 times the planet surface radius.

When the parking orbit is in the plane of the interplanetary trajectories, part or all of the required turning θ can result from the turning due to the gravity of the planet δ:

$$\delta = \delta_2 + \delta_3 \tag{22}$$

where δ_i is given by equation (19) (see also fig. 7(c), p. 10).

The greatest turning due to gravity occurs for the minimum periapsis $r_p = 1.1$. Values of δ for $r_p = 1.1$ are also plotted in figure 10. The δ decreases from near 155^o at the Hohmann leg time of 940 days to near 90^o for a leg time of 300 days. The θ and δ curves cross at leg time in the neighborhood of 530 days. The difference between this turning and the required turning θ is σ:

$$\sigma = \theta - \delta \tag{23}$$

A positive value of σ (T_o less than about 500 days) indicates that the turning due to gravity is insufficient. Similarly, a negative σ (T_o greater than about 570 days) indicates that there is an excess of gravity turning. The propulsive ΔV's and the type of parking orbit to be used depend on the sign of σ. The direction of rotation about Jupiter was chosen in every case to minimize $\sum \Delta V$.

Reference low circular orbit. - The reference parking orbit referred to previously is a circular orbit at 1.1 Jupiter radii (fig. 11(a)). This parking orbit is in the plane defined by Jupiter and the direction of $V_{\infty, 2}$ and $V_{\infty, 3}$. When the orbits of Jupiter and Earth are assumed coplanar, the parking orbit is in the plane of the planets. The ΔV to arrive at or leave this parking orbit is

$$\Delta V_i = V_{h,p} - V_c \tag{24}$$

where

$$V_{h,p} = \left(\frac{2\mu}{r_{h,p}} + V_\infty^2 \right)^{1/2} \tag{25}$$

and

$$V_c = \left(\frac{\mu}{r_c} \right)^{1/2} \tag{26}$$

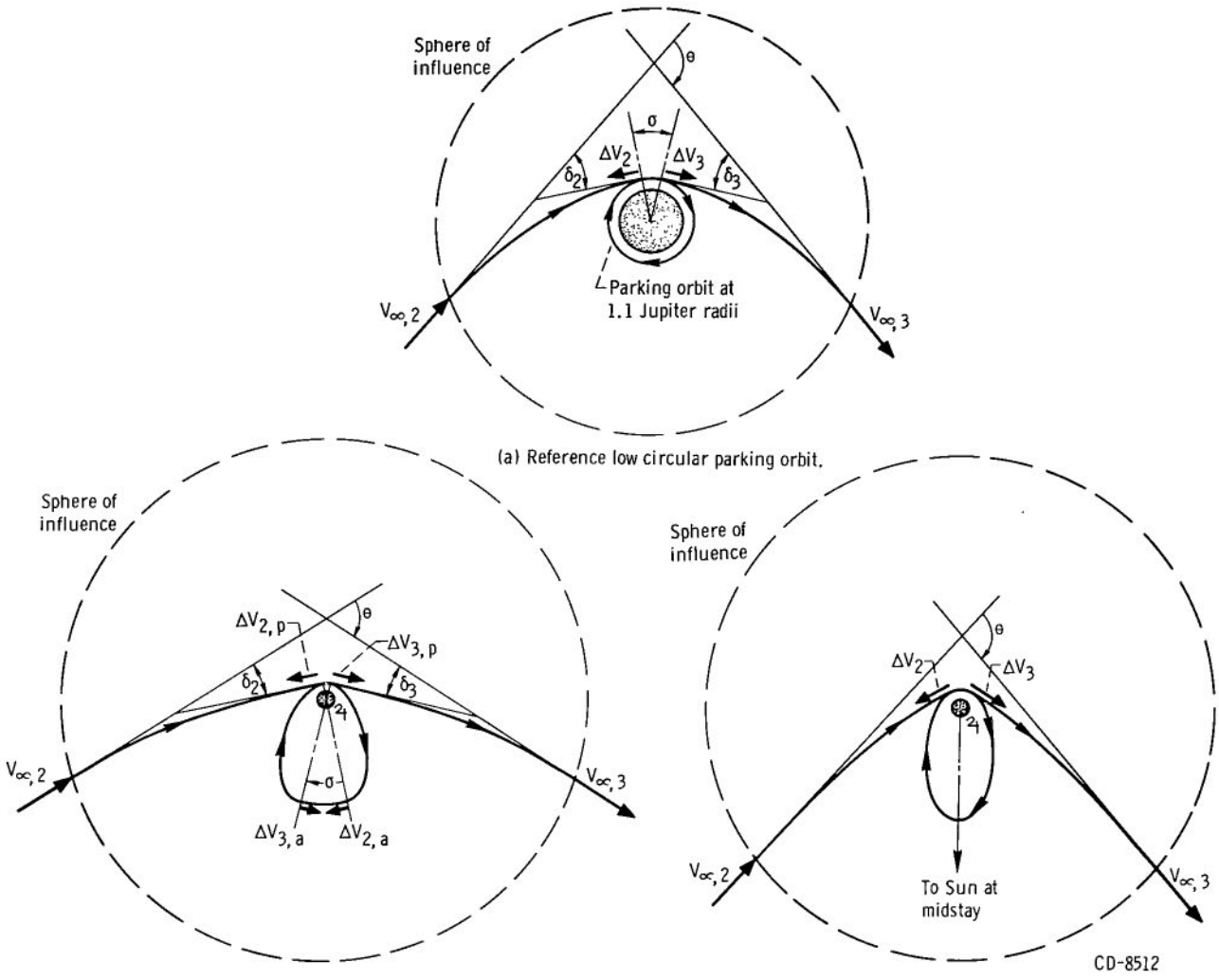

(a) Reference low circular parking orbit.

(b) Circularize-decircularize parking orbit.

(c) Elliptic parking orbit with off-periapsis thrusting.

Figure 11. - Jupiter parking orbits.

The period of the orbit is

$$T = 2\pi \left(\frac{r_c^3}{\mu} \right)^{1/2} \tag{27}$$

An advantage of the low circular orbit is that its period T is generally small compared with the stay time T_s. Thus, the time used to achieve the appropriate orientation for the departure hyperbola is negligible compared with the stay times or leg times, and there is no specific ΔV penalty to achieve the required reorientation.

The disadvantage of the low circular orbit is that the ΔV's to arrive and depart from

it are higher than for the following orbits.

Circularize-decircularize maneuver. - The circularize-decircularize maneuver shown in figure 11(b) occurs in the same plane as that of the circular orbit described previously. The spacecraft transfers from the hyperbolic approach trajectory to an elliptical trajectory at point 2. The approach hyperbola and parking ellipse are cotangential at their common apse which is at 1.1 Jupiter radii. The propulsive impulse is tangential and retrograde. At the apoapsis of the ellipse, point 2a, tangential and posigrade thrust sends the spacecraft into a circular orbit whose radius is the apoapsis radius of the ellipse. The turning angle σ is traversed in this high circular orbit to achieve the desired orientation for the departure. At point 3a, a tangential retrograde impulse places the space orbit in a second ellipse with the same values for the apses as the first ellipse. A tangential posigrade thrust at point 3 inserts the spacecraft into the Earth return trajectory. This parking orbit requires four impulses. The $\sum \Delta V$ is reduced from that needed for the circular reference orbit by an amount ΔV_s:

$$\Delta V_s = 2(V_{e,p} - V_{c1.1}) - 2(V_{c,a} - V_{e,a}) \tag{28}$$

The period of the parking orbit is

$$T = \pi\left\{N_e\left[\frac{(r_{e,p} + r_{e,a})^3}{2\mu}\right]^{1/2} + 2\left(\frac{r_{e,a}^3}{\mu}\right)^{1/2}\left(N_c + \frac{\sigma}{360}\right)\right\} \tag{29}$$

where N_c and N_e are the number of completed circular and elliptic orbits, respectively. For the type of orbit depicted in figure 11(b), $N_e = 1$ and $N_c = 0$.

Elliptic orbit with off-periapsis thrusting. - This elliptic orbit, which is shown in figure 11(c), is also in the plane of the planetary orbits. The parking ellipse has a periapsis of 1.1 Jupiter radii and its axis at midstay time or midtrip duration is the Jupiter-Sun line for a symmetrical round trip. The required relative orientations of the arrival and departure hyperbolas are obtained by arriving, point 2, and departing, point 3, from the parking ellipse at true anomaly angles different from zero. The true anomaly is chosen to minimize the propulsive ΔV. The parking orbit requires two nontangential thrusting impulses and can be used for either positive or negative values of σ. A systematic search over a range of true anomalies was made to find the ones yielding the minimum $\sum \Delta V$ while satisfying the boundary conditions.

Apo-twist. - The apo-twist parking orbit is shown in figure 11(d). In general, it lies in planes inclined to the plane of the planets. The first impulse, point B, to acquire the elliptical parking orbit is a cotangential retrograde thrusting at 1.1 Jupiter radii, which

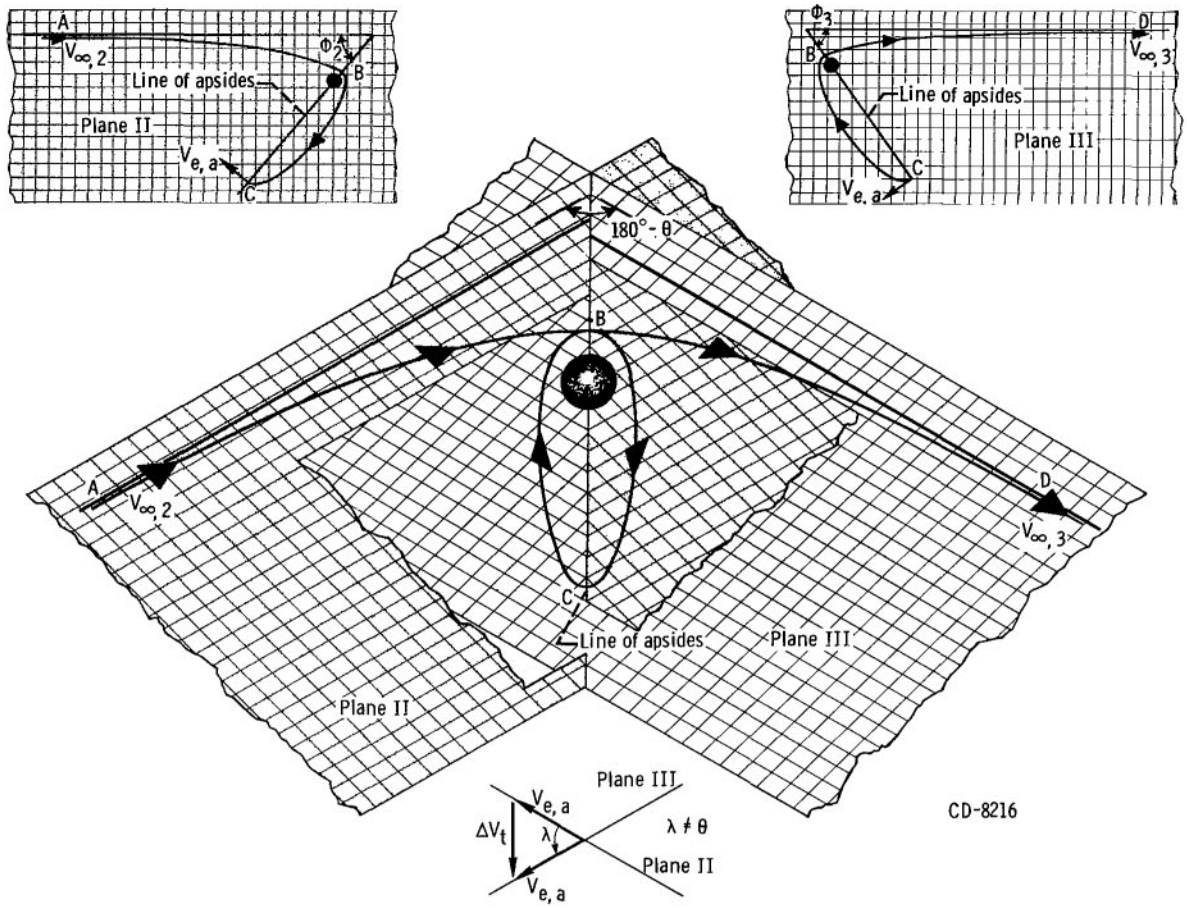

(d) Apo-twist parking orbit.

Figure 11. - Concluded.

is the common apse of the approach hyperbola and the initial semiellipse. At the apoapsis of the ellipse, point C, a second out-of-plane impulse is applied to twist the ellipse about its major axis without changing its orbit elements. The departure maneuver, point B, is similar to that of arrival. The spacial orientation of the ellipses and twist angle were chosen to satisfy the boundary conditions imposed by the arrival and departure hyperbolas. This parking orbit has three maneuvers and is applicable only when σ is positive.

The $\sum \Delta V$ is reduced from that needed for the circular reference orbit by an amount ΔV_s:

$$\Delta V_s = 2(V_{e,p} - V_{c1.1}) - 2V_{e,a} \sin \frac{\lambda}{2} \tag{30}$$

where λ is the twist angle. The period of the ellipse is

$$T = N_e \pi \left[\frac{(r_{e,a} + r_{e,p})^3}{2\mu} \right]^{1/2} \tag{31}$$

Nonstop Round Trips

For some nonstop round trips, the gravity of Jupiter provides the correct planetocentric turning θ; that is, σ has a value of zero. These nonstop trips can be accomplished without any propulsive effort required at Jupiter. For trips that yield a negative σ (fig. 10, p. 14), the gravity turning can be reduced by simply increasing the radius of periapsis passage. In this manner, σ can be made zero and no ΔV will be required as before. When gravity does not provide enough turning (σ positive), however, propulsion is required to generate part of the turning as illustrated in figure 12. Only symmetrical trips are considered for which $V_{\infty,2} = V_{\infty,3}$, $\beta_2 = \beta_3$, and $V'_{\infty,2} = V'_{\infty,3}$.

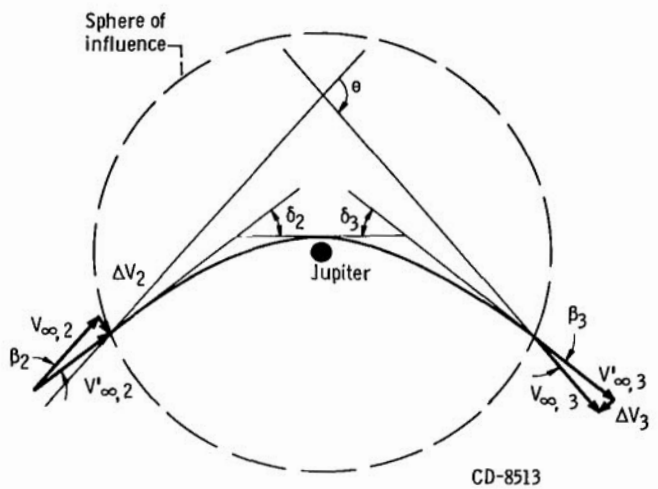

Figure 12. - Sphere of influence turning for round-trip nonstop trajectories.

The propulsive velocity increment at arrival ΔV_2 may both provide part of the total turning β_2 and reduce the hyperbolic excess velocity from $V_{\infty,2}$ to $V'_{\infty,2}$. This will increase the turning due to gravity δ_2. The ΔV_3 then also provides part of the turning $\beta_3 = \beta_2$ and increases $V'_{\infty,3}$ to $V_{\infty,3} = V_{\infty,2}$.

The total propulsive velocity increment required in the vicinity of Jupiter is, by symmetry,

$$\Delta V_2 + \Delta V_3 = 2\,\Delta V_2 \tag{32}$$

It is convenient to consider the problem further in velocities made dimensionless by dividing by the circular velocity at the trajectory periapsis:

$$\overline{V} = \frac{V}{V_{c1.1}} \tag{33}$$

where

$$V_{c1.1} = \left(\frac{\mu}{1.1\, r_2}\right)^{1/2} \approx 25.3 \text{ miles/sec} \tag{34}$$

Using the law of cosines gives

$$\Delta\bar{V}_2^2 = \bar{V}_{2,\infty}'^2 + \bar{V}_{2,\infty}^2 - 2\bar{V}_{2,\infty}\bar{V}_{2,\infty}' \cos\beta_2 \tag{35}$$

where from figure 12

$$\beta_2 = \frac{\theta - 2\delta_2}{2} \tag{36}$$

and

$$\delta_2 = \sin^{-1}\frac{1}{\left(\bar{V}_{2,\infty}'\right)^2 + 1} \tag{37}$$

Differentiating equation (35) with respect to β_2 (with θ and $V_{\infty,2}$ held constant) and setting the result equal to zero give a relation between $\bar{V}_{\infty,2}'$ and β_2 for a minimum ΔV_2:

$$\bar{V}_{\infty,2}' = \bar{V}_{\infty,2}\cos\beta_2\left\{1 - \frac{2\left[1 - \sin\left(\frac{\theta - 2\beta_2}{2}\right)\right]\sin\left(\frac{\theta - 2\beta_2}{2}\right)\tan\beta_2}{\cos\left(\frac{\theta - 2\beta_2}{2}\right)}\right\} \tag{38}$$

Equations (35), (36), and (38) may be solved simultaneously to give $\beta_{2,\text{opt}}$ as a function of θ and $V_{\infty,2}$. When $\beta_{2,\text{opt}}$ is known, equations (38) and (35) yield the minimum ΔV_2.

The method just described is an optimum two-impulse sphere of influence turning maneuver. However, a round trip for positive σ's can also be accomplished if a single impulse is used at either the arrival or departure sphere of influence. The total ΔV for this maneuver is

$$\Delta V = 2V_{\infty,2}\sin\left(\frac{\sigma}{2}\right) \tag{39}$$

A more general discussion of optimized deflected trajectories is given in reference 10.

Out-of-Ecliptic Trajectories to Jupiter

The interplanetary trajectories considered thus far all consist of legs that are a single conic lying in the ecliptic plane. However, for missions to Jupiter it may be advantageous to travel out of the ecliptic plane to minimize hazards posed by passing through the center of the asteroid belt. The greatest density of asteroids lies in the ecliptic plane at a distance of about 2.8 astronomical units from the Sun. An out-of-ecliptic mission can be accomplished by employing either a single- or broken-plane Earth to Jupiter transfer as shown in figures 13(a) and (b), respectively.

For an out-of-ecliptic mission, the Earth departure is made so that some desired altitude from the ecliptic H is achieved at the radius R from the Sun. If the broken plane transfer is being used, a ΔV is applied at the point of maximum H to put the vehicle on an intercept trajectory with the target planet. The travel angle ψ_o is 180^o if a single-plane transfer is used.

A simplified analysis of the problem was made by assuming that $H/R \ll 1.0$ so that the elements of the transfer conic remain essentially unchanged.

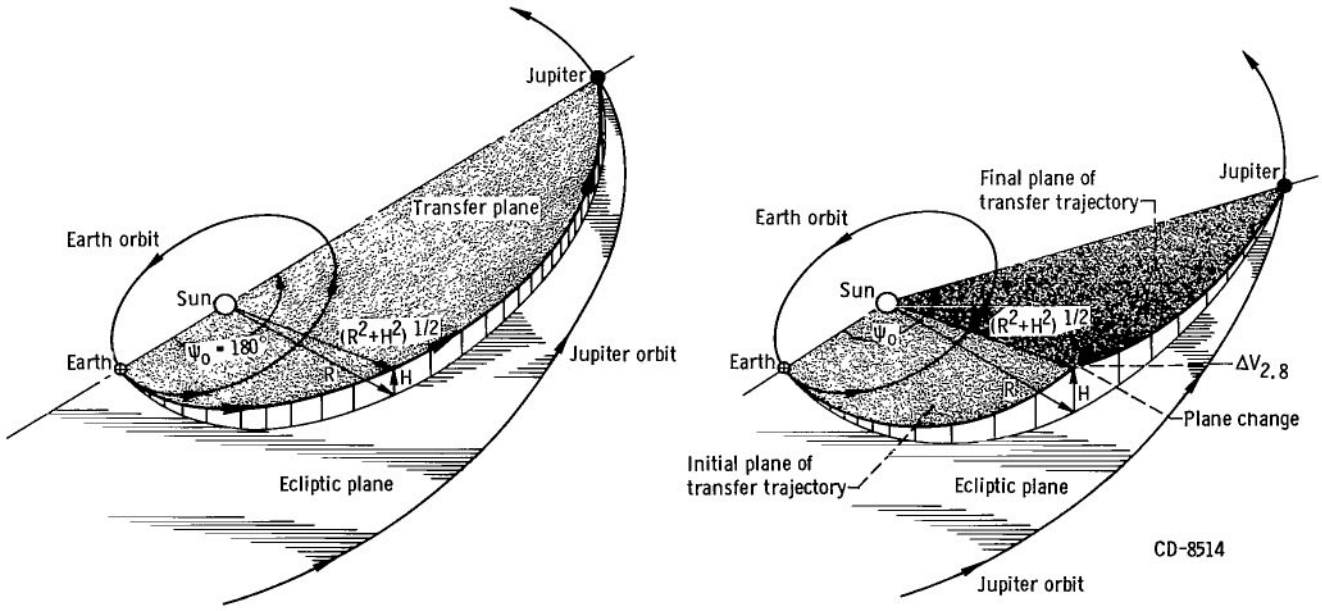

(a) Single plane transfer, $\psi_o = 180°$.

(b) Broken plane transfer, $\psi_o \neq 180°$.

Figure 13. - Out-of-ecliptic Earth to Jupiter trajectory.

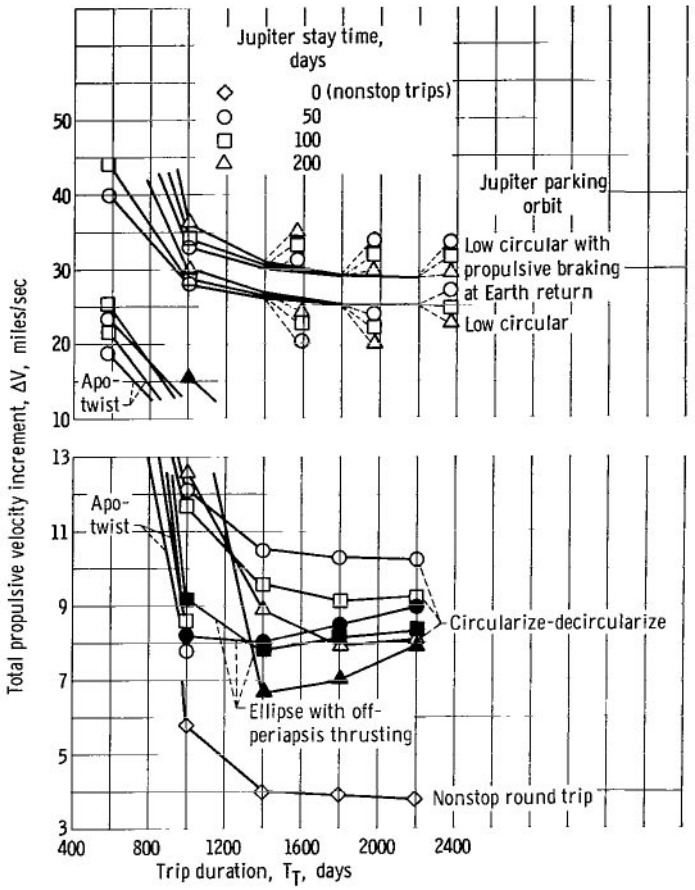

Figure 14. - Variation of total propulsive velocity increment for Jupiter round trips with trip duration, stay time, profile, and parking orbit. All trips use minimum ($\Delta V_1 + \Delta V_2$) symmetric trajectories. (Atmospheric braking at Earth return except where noted.)

RESULTS AND DISCUSSION

The propulsive velocity increments for symmetrical round trips to Jupiter are plotted against mission duration in figure 14. The data points represent discrete local minimums. These points are connected with straight line segments only for the purpose of identifying trajectories with common characteristics. For the stopover trajectories, stay times of 50, 100, and 200 days are presented. The stay time for the nonstop trips is, of course, zero.

As a whole, the curves for each of the parking orbits show a modest increase in $\sum \Delta V$ with decreasing trip duration from 2200 to 1000 days. A further decrease to 600 days results in a marked increase in $\sum \Delta V$. For this reason the 1000-day trip is an interesting one, and it is used in later discussions to illustrate the effect of several trajectory variations.

The following sections discuss in detail the effects shown in figure 14.

Effect of Atmosphere Braking

The upper two sets of curves in figure 14 show the effect of atmospheric braking on the total mission ΔV if a low circular parking orbit is used at Jupiter. The uppermost set uses propulsive braking at Earth return, the lower set uses full atmospheric braking at Earth return. The effect of using atmospheric braking is to reduce the total mission ΔV by 4 miles per second for the longer trips and 10 miles per second for the 600-day trip.

The corresponding Earth approach velocities are shown in figure 15. These are the atmospheric entry velocities if no supplemental propulsive deceleration is used. For trip durations of 1000 days and longer, the entry velocities are less than about 10.5 miles per second or they are about twice the circular orbital velocity at 1.1 Earth radii. This

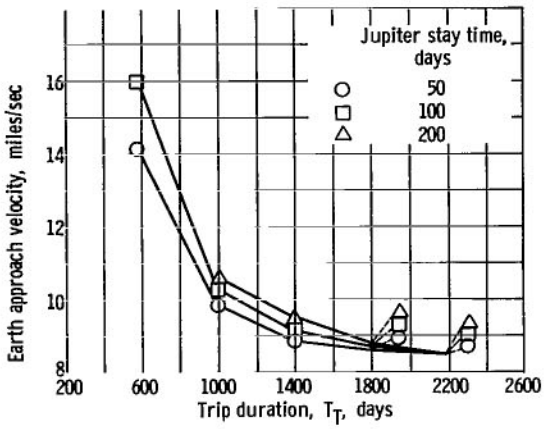

Figure 15. - Variation of Earth approach velocity with trip duration and stay time. All trips use minimum $(\Delta V_1 + \Delta V_2)$ symmetric trajectories.

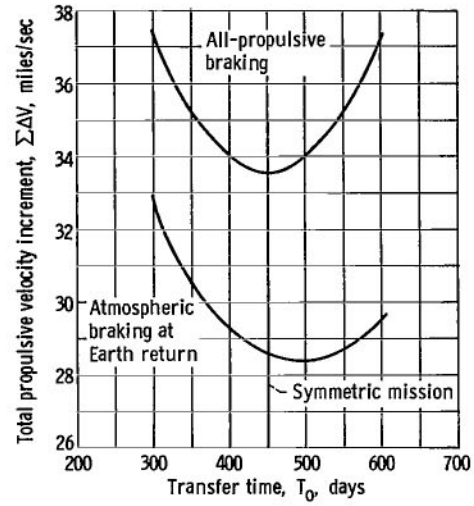

Figure 16. - Effect of atmospheric braking at Earth return on variation of total propulsive velocity increment with outbound leg time. Trip duration, 1000 days; stay time, 100 days.

is within the range of estimated future feasibility.

Atmospheric braking at Jupiter was not considered because of the very high approach velocities, that is, 45 miles per second or about 10 times the circular orbital velocity at 1.1 Earth radii.

Figure 16 shows the variation of $\sum \Delta V$ with outbound leg time for trips of 1000-day duration and 100-day stay. It was argued in the METHOD OF ANALYSIS section that for all-propulsive trips symmetrical trajectories should give the lowest $\sum_{n=1}^{4} \Delta V_n$. This point is illustrated by the upper curve. The outbound leg time for the symmetrical trip is 450 days.

When atmospheric braking is used and if there is no restriction on the Earth approach velocity, then a minimum $\sum_{n=1}^{3} \Delta V_n$ is desirable. In this case, symmetrical trips no longer yield the minimum $\sum_{n=1}^{3} \Delta V_n$ as illustrated by the lower curve. A $\sum \Delta V$ of 0.2 mile per second less than that for a symmetrical trip is possible by increasing the outbound leg time from 450 to 500 days. The increase in Earth approach velocity is about 0.4 mile per second.

The following results use atmospheric braking at Earth return and are symmetrical trips. A slight reduction, like 0.2 mile per second, from the $\sum \Delta V$'s shown is thus possible.

Effect of Parking Orbit Type and Stay Time

This section presents in detail the ΔV requirements of each parking orbit discussed in the METHOD OF ANALYSIS section. The period of each elliptic parking orbit is assumed to equal the stay time.

Low circular parking orbit. - This parking orbit was used to show the advantage of atmospheric over propulsive braking at Earth return. As mentioned before, the second set of curves on figure 14 shows the total mission ΔV for the low circular parking orbit with atmospheric braking. The individual ΔV's for this trip may be determined from the data of figure 3 (p. 7). The ΔV_1 and ΔV_4 ($\Delta V_1 = \Delta V_4$ for symmetrical trips) thus determined are common to all mission profiles with the same trip duration and stay time.

For the low circular parking orbit, the effect of stay time on mission ΔV is quite small for trips of 1000 days or longer (fig. 14). However, for shorter trips an appreciable ΔV penalty is incurred in increasing the stay time from 50 to 200 days.

Circularize-decircularize parking orbit. - It can also be seen in figure 14 that using a circularize-decircularize parking orbit (depicted in fig. 11(b), p. 16) reduces the $\sum \Delta V$ to about half that for a low circular parking orbit. The individual ΔV's for the maneuvers at Jupiter for this parking orbit are given in figure 17. It must be remembered that the period of the parking orbit is equal to the stay time; that is, there are no integral revolutions in the high circle or in the ellipse. For trips of 1000 days and longer, the ΔV's for the maneuvers at the apoapsis of the parking orbit, $\Delta V_{2,a}$ and $\Delta V_{3,a}$, are larger than the ΔV's for the maneuvers to arrive at and depart Jupiter, $\Delta V_{2,p}$ and $\Delta V_{3,p}$. The magnitudes of $\Delta V_{2,a}$ and $\Delta V_{3,a}$ decrease with longer stay times, and this accounts for the variation with stay time shown in figure 14, that is, that longer stay times give lower $\sum \Delta V$ for $T_T \geq$ 1000 days.

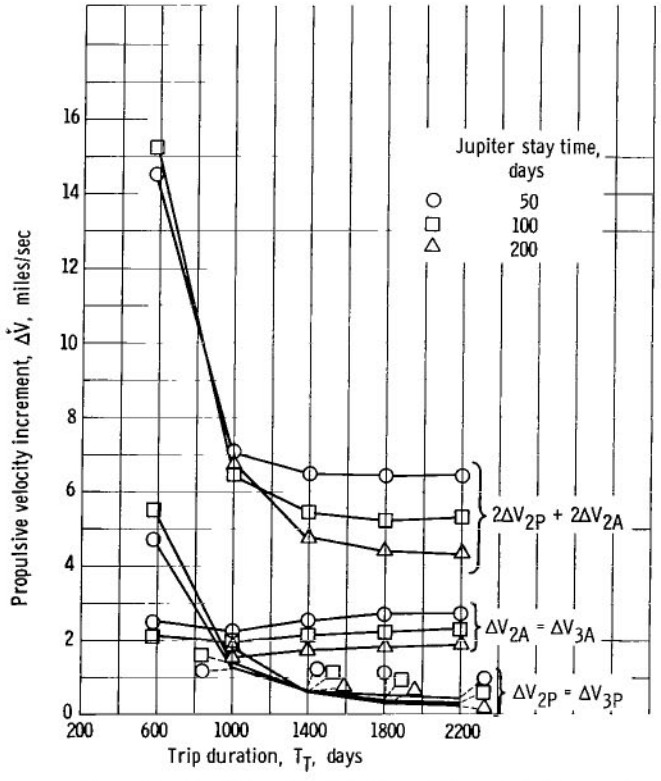

Figure 17. - Variation of individual propulsive velocity increments with trip duration and stay time for circularize-decircularize parking orbit. All trips use minimum ($\Delta V_1 + \Delta V_2$) symmetric trajectories. Direct motion parking orbits for 1400- and 1800-day trips, others retrograde.

Ellipse with off-periapsis thrusting. - Figure 14 shows that a still further reduction in $\sum \Delta V$ can be obtained by using the elliptical parking orbit with off-periapsis

thrusting. For the 1000-day trip, this parking orbit requires from 2.6 to 3.6 miles per second less propulsive effort than the previous case. At trip times shorter than 1000 days, the ΔV requirement increases rapidly and the advantage of this maneuver is lost. The individual ΔV's for this parking orbit are shown in figure 18. Compared with the circularize-decircularize orbit, the high values of $\Delta V_{2,a}$ and $\Delta V_{3,a}$ are eliminated altogether and the values of ΔV_2 and ΔV_3 have increased modestly over the values of $\Delta V_{2,p}$ and $\Delta V_{3,p}$, giving a net reduction in $\sum \Delta V$.

The effect of the parking ellipse orientation on propulsion requirements is shown in figure 19. The preceding results were for a symmetrically oriented ellipse indicated by the center sketch. This orientation yields the lowest $\Delta V_2 + \Delta V_3$ as the curve shows. The distribution in ΔV between ΔV_2 and ΔV_3 is strongly affected by the ellipse orientation, while the ΔV sum is affected only 0.5 out of 3.9 miles per second. For a mission that has a large payload jettisoned at Jupiter, for instance, the Jupiter exploration

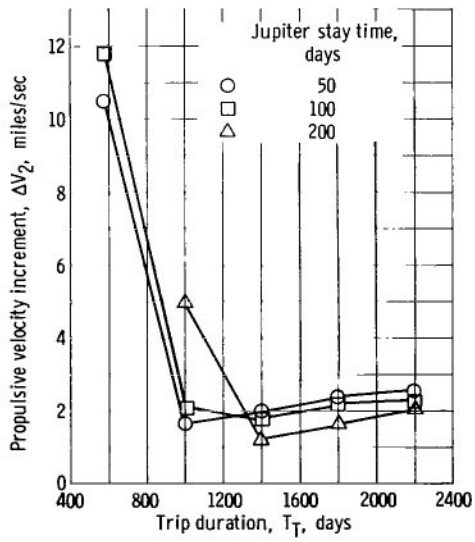

Figure 18. - Variation of propulsive velocity increments with trip duration and stay time for elliptic parking orbit with off-periapsis thrusting. All trips use minimum (ΔV_1 + ΔV_2) symmetric trajectories. Direct motion parking orbit for 2200-day trip, others retrograde.

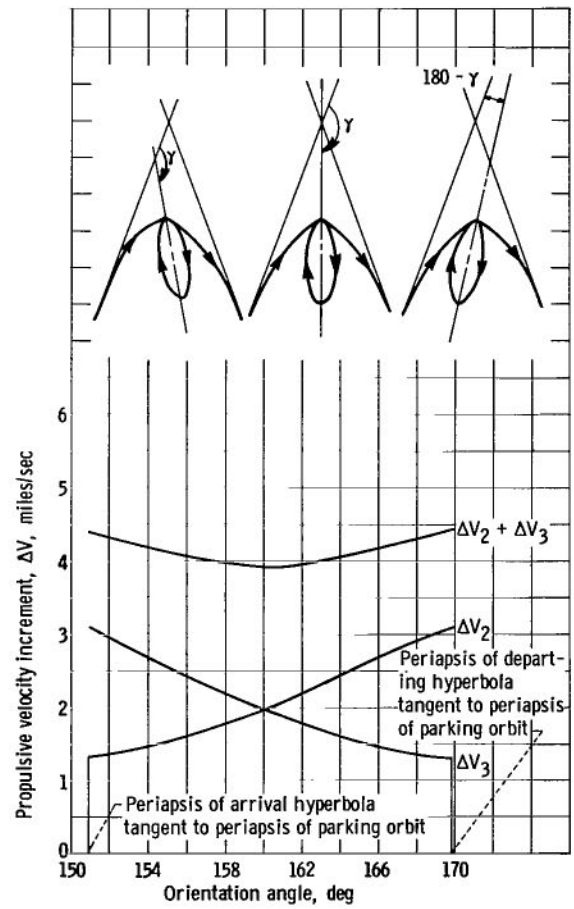

Figure 19. - Effect of ellipse orientation on propulsive velocity increments for elliptic parking orbit with off-periapsis thrusting. Trip duration, 1000 days; stay time, 100 days; symmetric interplanetary legs.

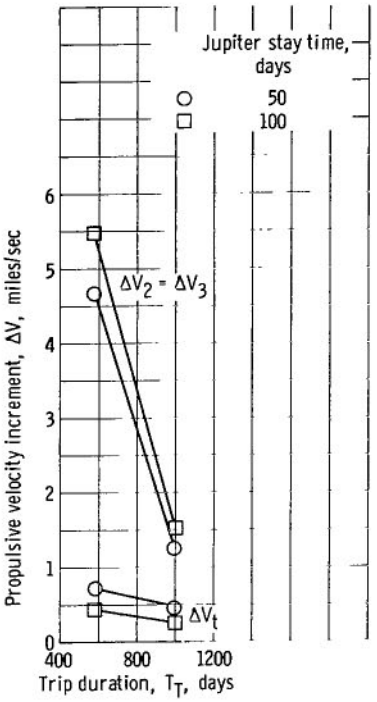

Figure 20. - Variation of individual propulsive velocity increments with trip duration and stay time for apo-twist parking orbit. All trips use minimum ($\Delta V_1 + \Delta V_2$) symmetric trajectories.

system weights, the minimum initial weight in Earth orbit will tend to occur for the trajectory with the lower ΔV_2 and the higher ΔV_3, providing the sum of ΔV_2 and ΔV_3 is about the same. This situation exists with the ellipse oriented so that the arrival is near the ellipse periapsis (see the sketch on the left in fig. 19).

Apo-twist parking orbit. - The apo-twist parking orbit, depicted in figure 11(d) (p. 18), is applicable only when the turning angle σ is positive, which for symmetrical trips corresponds to leg times less than about 500 days (fig. 10, p. 14). It thus applies for trip durations of 1000 and 600 days. For the 1000-day trip with a 100-day stay (fig. 14, p. 22), the apo-twist maneuver yields a $\sum\Delta V$ of about 8.5 miles per second, or 0.7 miles per second less than the ellipse with off-periapsis thrusting. For the 600- and 1000-day stopover trips, this parking orbit gives the lowest $\sum\Delta V$ of the ones considered. For the 1000-day trip, the mission $\sum\Delta V$ using the apo-twist parking orbit is one-fourth of that for the low circular orbit. This parking orbit is oriented out of the plane of the moons and hence may not be convenient as a parking orbit from which to launch excursions to the moons.

The individual maneuver ΔV's are shown in figure 20. The twist velocity increment ΔV_t, which is the penalty for achieving the required orientation of the ellipse, is about 0.5 mile per second, a low value. The values of ΔV_2 and ΔV_3 are for arriving or departing from the ellipse periapsis with tangential thrusting.

Effect of stay time on mission ΔV. - The elliptic parking orbits discussed all show the same general characteristics with increasing stay time. At the longer trip times, $T_T \geq 1400$ days, longer stay times tend to yield the lower $\sum\Delta V$. The longer period ellipses have higher energies and consequently require lower ΔV's for the arrival-departure maneuvers. The opposite trend occurs for the shorter trip durations in that longer stay times increase the $\sum\Delta V$. Longer stay times mean decreased leg times. The increase in ΔV associated with shorter leg times (fig. 3, p. 7) outweighs the previously mentioned trend of decreasing ΔV with longer elliptic periods that predominates at the longer trip times.

Effect of parking orbit period on mission $\sum\Delta V$. - All the preceding elliptic parking orbit data are for the case where the period of the parking orbit is equal to the stay time. The effect of an elliptic parking orbit with periods less than the stay time is shown in figures 21 and 22. The 1000-day round trip with a stay time of 100 days is used for illustration. The periapsis of the ellipse is fixed at 1.1 Jupiter radii.

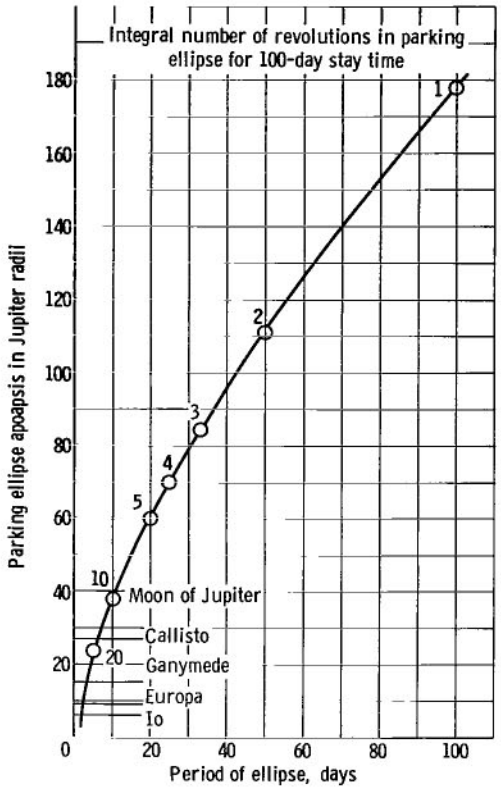

Figure 21. - Effect of parking ellipse period on apoapsis radius. Parking ellipse periapsis at 1.1 Jupiter radii.

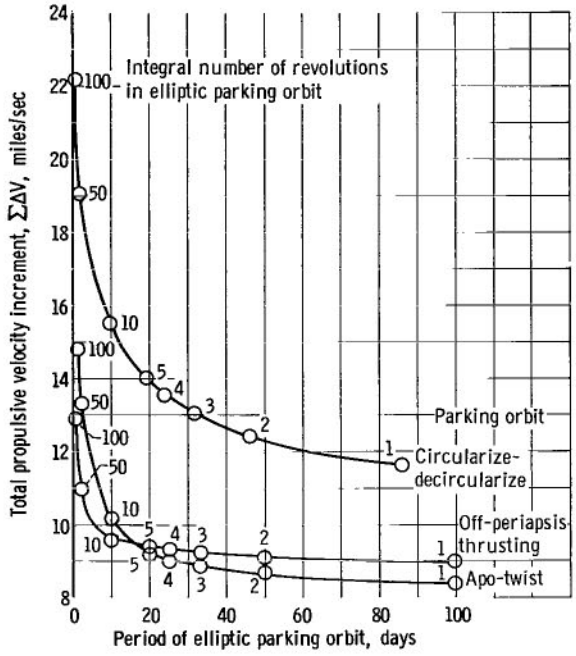

Figure 22. - Effect of elliptic parking orbit period on total mission propulsive requirement. All trips use minimum ($\Delta V_1 + \Delta V_2$) symmetric trajectories; trip duration, 1000 days; stay time, 100 days; parking ellipse periapsis at 1.1 Jupiter radii.

Figure 21 presents the elliptic apoapsis radius as a function of the elliptic period. For an ellipse with a 100-day period the apoapsis is at 179 Jupiter radii. (As a point of interest, the Jupiter sphere of influence is at about 600 radii.) The ellipse periapsis decreases rapidly with decreasing period, for instance, to 38 radii at a period of 10 days. The radii of some of the moons of Jupiter are also noted on the curve for comparison. The ellipse with a 7-day period has an apoapsis at about the same radius as Callisto and hence may be of interest. The other moons are at still lower radii.

Figure 22 shows the mission $\sum \Delta V$ as a function of elliptic period for the 1000-day trip using circularize-decircularize, ellipse with off-periapsis thrusting and the apo-twist parking orbits. Integral number of revolutions in the elliptic orbit are noted on each curve. The circularize-decircularize curve is shifted to the left due to the time required to accomplish the turning angle σ in the high circular orbit.

For the 1000-day trip, the apo-twist parking orbit gives the lowest $\sum \Delta V$ over a broad range of ellipse periods. However, the fire-off-periapsis maneuver is least affected by a reduction in the elliptic period. For instance, the percentage increases in mission $\sum \Delta V$ required to go to a 10-day from a 100-day ellipse at Jupiter (but with a

100-day stay in all cases) is 6.7, 21, and 32 percent for the fire-off periapsis, apo-twist and circularize-decircularize parking orbits, respectively. At ellipse periods less than about 16 days, corresponding to low apoapsis radius, the ellipse with off-periapsis thrusting yields a lower ΔV than the apo-twist maneuver.

Nonstop round trips. - For trips of 1000 days and longer, the nonstop trips give lower $\sum \Delta V$'s than the stopover trips (fig. 14, p. 22). For trips of 1400 days and longer, the ΔV is about 4 miles per second, about half that for the best stopover trips. For these trips the gravity of Jupiter alone provides adequate turning. The only propulsion for the trip is that to depart Earth ΔV_1. The desired turning at Jupiter is achieved by the selection of the periapsis of the encounter hyperbola. The periapsis radii are given in figure 23. For the 1400-day trip the value is 9.9 Jupiter radii.

For the 1000-day trip, propulsive turning in addition to the turning due to gravity of Jupiter is required (as depicted in fig. 12, p. 19). The periapsis is 1.1 radii and the $\sum \Delta V$ is now 6.0 miles per second, about 2.5 miles per second less than for the best 100-day-stay stopover trip (fig. 14). The magnitudes of the propulsive maneuvers required near Jupiter depend on the periapsis of Jupiter passage, and the eccentricities

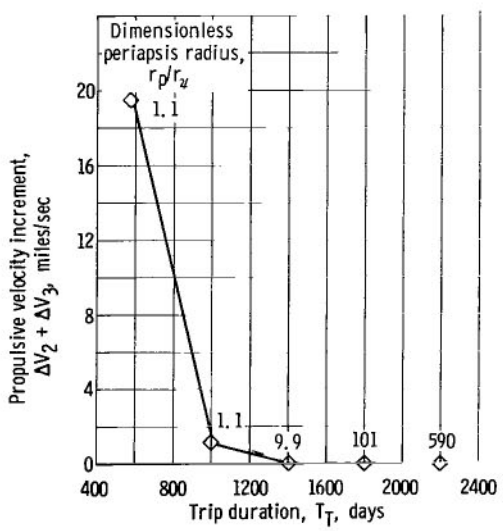

Figure 23. - Variation of propulsive velocity increment required at Jupiter and radius of periapsis passage with mission duration for nonstop round trips.

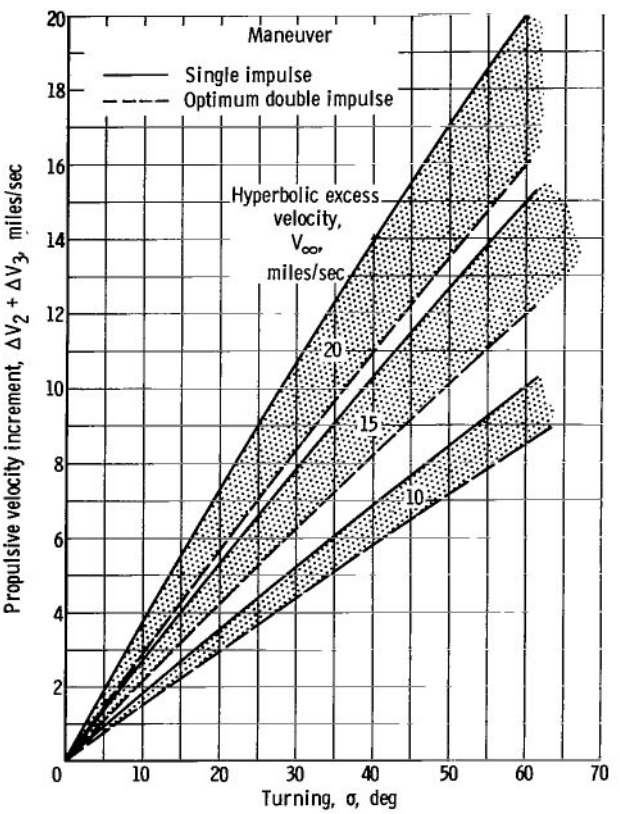

Figure 24. - Variation of velocity increment required at Jupiter with turning and hyperbolic excess velocity for optimum double- and single-impulse sphere-of-influence turning maneuvers.

and inclinations of the planetary orbits which are here assumed zero. For the 580-day nonstop round trip the $\sum \Delta V$ is greater than that for the stopover trip.

The propulsive ΔV required at Jupiter for the nonstop trips is also shown in figure 23. The ΔV is zero for trips of 1400 days and longer. At 1000 days and shorter, the ΔV was found using the optimum two-impulse symmetric sphere-of-influence turning maneuver.

A comparison of the optimum two-impulse symmetrical maneuver and the single-impulse maneuver (see METHOD OF ANALYSIS, Nonstop Round Trips) is shown in figure 24. The ΔV required at Jupiter for symmetrical trips is plotted against the turning σ for each maneuver. Three typical hyperbolic excess velocities are shown. It is apparent from this figure that an appreciable reduction in mission ΔV is possible in going from the single-impulse to the optimum double-impulse maneuver at the sphere of influence.

Out-of-ecliptic trajectories. - The 1000-day trip with a 100-day stay time is used to illustrate the broken-plane out-of-ecliptic Earth to Jupiter transfer shown in figure 13(b) (p. 21). The ΔV penalty associated with flying this mission is plotted in figure 25(a) against distance out of the ecliptic. For this example, R = 2.8 astronomical units and a low circular parking orbit is used at Jupiter. This figure shows that the ΔV penalty is approximately linear with H and reaches a value of 6.7 miles per second at an altitude of 0.5 astronomical unit from the ecliptic. The largest part of the ΔV penalty is for the

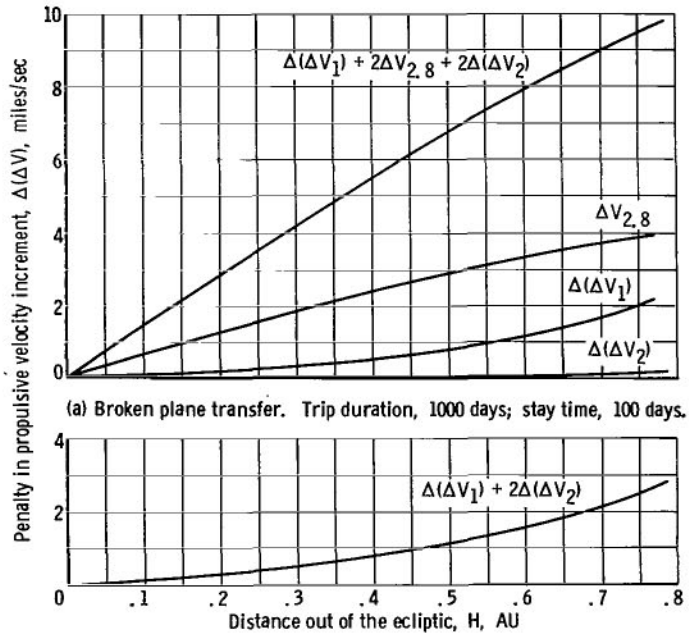

Figure 25. - Variation of propulsive penalty with distance out of the ecliptic. Distance measured at 2.8 astronomical units from the Sun.

ΔV to change planes at 2.8 astronomical units. This represents an increase in mission ΔV of 84 percent if the apo-twist parking orbit is used at Jupiter and an increase of 24 percent if the low circular parking orbit is used. It is apparent that for this mission an appreciable ΔV penalty can be involved with flying out of the ecliptic.

A trajectory that passes the same distance H above the ecliptic plane at R = 2.8 astronomical units is possible with no ΔV at 2.8 astronomical units if a 180° transfer leg is used. This is a single-plane transfer. The trajectory with a minimum $\Delta V_1 + \Delta V_2$ for a 180° transfer is the Hohmann semiellipse. The round trip made up of an outbound and inbound leg of Hohmann transfers has a total trip duration of 2200 days and a stay time of about 315 days. The ΔV penalty for traveling out of the ecliptic for this trip is shown in figure 25(b). It is much smaller than for the 1000-day trip, about 1.2 miles per second at H = 0.5 astronomical unit. For leg times less than the Hohmann leg time the ΔV penalty for the single-plane out-of-ecliptic trajectory will increase and is expected to be comparable to that for the broken-plane transfer for the 1000-day trip.

Rendezvous at Jupiter

The possible use of rendezvous at Jupiter is illustrated in figure 26. This trip differs from the conventional ones in that three separate crafts depart Earth. The first craft

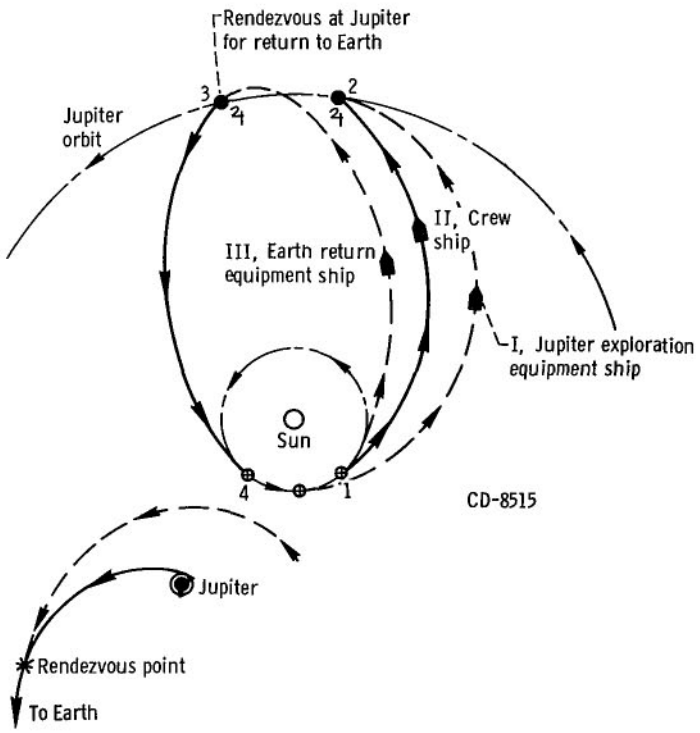

Figure 26. - Jupiter rendezvous round trip.

contains that part of the mission equipment required in Jupiter orbit, such as the Jupiter exploration equipment and part of the life-support weight. This craft is sent on a low-energy longer-leg-time trajectory than that for the crew ship. To have the equipment at Jupiter when the crew arrives, this craft must depart about 13 months before the crew.

The second craft is the crew ship; it travels the stopover round trip. For this example a 1000-day trip with a 100-day stay, and an elliptical parking orbit with off-periapsis thrusting is used. This parking orbit was chosen because the Jupiter rendezvous is more advantageous with this parking orbit. Also this parking orbit may be a favorable one for the exploration of the Jupiter moons.

The third craft carries the Earth deceleration system and the return leg life-support weight. It flies a nonstop round-trip trajectory with a return leg coincident with the return leg of the stopover trajectory. The departure from Earth may occur a month after the crew ship.

The propulsion requirements described for the three crafts are shown in table II. The $\sum \Delta V$ for the Jupiter exploration equipment, $\Delta V_1 + \Delta V_2$, has been reduced from a value of 9.2 (if this equipment is carried with the crew) to 5.5 miles per second. The $\sum \Delta V$ of the Earth return equipment has been reduced from 9.2 to 6.0 miles per second.

Depending on the mass carried in each phase of the mission, the reductions in $\sum \Delta V$ for two phases of the mission can result in a significant saving in initial mass in Earth orbit. This has been but an example of what can be done with multiple-phase rendezvous

TABLE II. - PROPULSION REQUIREMENTS FOR JUPITER RENDEZVOUS

TRIP CREW TRAJECTORY

[Trip duration, 1000 days; stay time, 100 days; elliptical parking orbit with off-periapsis thrusting.]

Propulsion required	I Jupiter exploration equipment ship	II Crew ship	III Earth return equipment ship
	One way trajectory, ~790 day out-bound leg (100-day orbit), miles/sec	Stopover trajectory (round-trip 100-day orbit), miles/sec	Nonstop trajectory (round-trip zero stay), miles/sec
ΔV_1	~4.0	5.2	4.8
ΔV_2	~1.5	2.0	.6
ΔV_3	----	2.0	.6
ΔV_4 (atmospheric braking)	----	0	0
Total propulsion required	~5.5	9.2	6.0

mission profiles. Similar profiles can be constructed for other trip durations. A detailed mission analysis is required to evaluate the relative merits of the possible mission profiles.

Effect of Circular Coplanar Assumption

The trajectories discussed thus far were all evaluated by assuming that Earth and Jupiter lie in circular coplanar orbits about the Sun. This assumption makes truly symmetrical missions possible. In order to test the accuracy of the results obtained with this assumption, several representative Earth to Jupiter trajectories including the effect of orbital eccentricity and inclination were calculated. The results (in terms of mission ΔV's) are shown in table III. Earth launch dates in the 1983 to 1992 time period are considered. The ΔV's calculated assuming circular coplanar orbits are within 5 percent of those found if allowance is made for eccentricity and inclination, and the present assumptions give ΔV values higher than those in the average year.

TABLE III. - EFFECT OF PLANETARY ORBIT ECCENTRICITY AND INCLINATION ON PROPULSIVE REQUIREMENTS

[Low circular parking orbit at Jupiter; outbound leg time, ~490 days; departure date selected for minimum $\Delta V_1 + \Delta V_2$.]

	Propulsive velocity increments, ΔV, miles/sec	
	Earth departure, ΔV_1	Jupiter arrival, ΔV_2
Circular coplanar (present assumptions)	4.86	11.47
Elliptic noncoplanar		
1983	4.64	11.41
1985	4.52	11.22
1987	4.54	11.18
1989	4.76	11.33
1992	4.88	11.47

Comparison of Jupiter and Mars Trips

It was suggested in the INTRODUCTION section that trips to Jupiter can require much more propulsive effort than trips to Mars. This comparison was arrived at by consider-

TABLE IV. - COMPARISON OF PROPULSION REQUIREMENTS FOR MARS AND JUPITER ROUND TRIPS

Destination	Mission profile	Propulsive velocity increments, ΔV, miles/sec					
		Leaving Earth, ΔV_1	Arriving destination, ΔV_2	Parking orbit, ΔV_t	Leaving destination, ΔV_3	Arriving Earth, ΔV_4	Total
Mars	420-Day duration 40-Day stay Low circular parking orbit:						
	All propulsive	2.56	2.58	----	3.75	7.82	16.8
	Atmospheric braking at Earth return	2.56	2.58	----	3.75	---	9.0
Mars	1000-Day duration 450-Day stay Low circular parking orbit:						
	All propulsive	2.17	1.44	----	1.45	2.59	7.7
	Atmospheric braking at Earth return	2.17	1.44	----	1.45	----	5.06
Jupiter	1000-Day duration 100-Day stay Apo-twist parking orbit:						
	Atmospheric braking at Earth return	5.2	1.50	0.25	1.50	---	8.45

ing trips with all-propulsive maneuvers and with low circular parking orbits at both Mars and Jupiter. However, the comparison changes markedly if an elliptical parking orbit is used at Jupiter along with atmosphere braking at Earth return.

The ΔV requirement for the 1000-day Jupiter trip using the apo-twist parking orbit with atmospheric braking at Earth return is shown in table IV. Several typical Mars trips are also shown. For the examples selected, the Jupiter round trips show mission ΔV's and trip durations comparable to those that are being considered for Mars.

SUMMARY OF RESULTS

The propulsive requirements for nonstop and stopover symmetrical round trips to Jupiter were obtained for a number of mission durations and Jupiter stay times. Total trip times of 500 to 2200 days and stay times of 0 to 200 days were considered. Methods employed to reduce the mission $\sum \Delta V$ include optimized heliocentric travel angles, atmospheric braking at Earth return, use of loosely captured elliptical parking orbits at

Jupiter, and rendezvous at Jupiter. Also investigated was the ΔV penalty associated with Earth to Jupiter transfer trajectories lying out of the plane of the ecliptic. All velocity changes were obtained impulsively and the assumption was made that Earth and Jupiter lie in circular coplanar orbits. The following results were obtained:

1. The mission $\sum \Delta V$'s calculated assuming circular coplanar planetary orbits are within 5 percent of those found if allowance is made for eccentricity and inclination.

2. The trajectories with the lowest propulsive velocity increment sum occurred for symmetrical trips (i. e., the heliocentric travel angle and the travel time were the same for the inbound and outbound legs). Symmetrical trips with local minimums in $\sum \Delta V$ occur in narrow bands of trip durations at intervals of about 400 days between trip durations of 600 and 2200 days.

3. For stopover trips, the mission ΔV can be reduced by nearly a factor of 4 if elliptical parking orbits are used at Jupiter in place of a low circular one. For instance, the ΔV for the 1000-day trip with a 100-day stay is reduced from 28 to 8 miles per second by changing from a low circular parking orbit at Jupiter to the apo-twist orbit.

4. Atmospheric braking at Earth return (assuming this capability exists) reduces the total mission ΔV by an additional 4 to 10 miles per second.

5. At trip times of 1400 days and greater, nonstop round trips can be made with about half the propulsive effort required for the most favorable stopover trip.

6. An appreciable ΔV increase can be incurred in using nonecliptic Earth to Jupiter transfers. For example, to obtain an altitude of 0. 5 astronomical unit from the ecliptic at 2. 8 astronomical units from the Sun, the ΔV penalty is 6. 7 miles per second for the 1000-day mission. For missions made up of Hohmann legs with 180^{o} transfers, the ΔV penalty can be much less but the mission times are very long.

7. The Jupiter rendezvous mission profile can yield significant reductions in propulsive effort for portions of the mission mass.

8. If the ΔV reducing techniques outlined in this report are used, stopover round trips to Jupiter can be made with about the same propulsive effort commonly considered for trips to Mars. The most favorable 1000-day trip to Jupiter requires a total $\sum \Delta V$ of about 8. 5 miles per second. This compares favorably with a $\sum \Delta V$ of 9. 0 miles per second found for a typical Mars mission.

Lewis Research Center,
National Aeronautics and Space Administration,
Cleveland, Ohio, April 28, 1966,
121-30-02-01-22.

APPENDIX - SYMBOLS

e	eccentricity
H	distance measured normal to ecliptic plane, AU
N_c	integral number of revolutions in parking circle
N_e	integral number of revolutions in parking ellipse
$N_\oplus$	integral number of revolutions of Earth about the Sun during trip
p	semilatus rectum, miles
R	radial distance from Sun, AU
r	radius of trajectory, miles
r_∞	radius of sphere of influence, miles
T	time
V	trajectory velocity, miles/sec
V_H	velocity of interplanetary trajectory in heliocentric coordinates at Jupiter sphere of influence, miles/sec
$V_{\mathcal{4}}$	velocity of Jupiter in its orbit about the Sun, miles/sec
V_∞	hyperbolic excess velocity, in planetocentric coordinates, located at sphere of influence, miles/sec
ΔV	propulsive velocity increment, miles/sec
ΔV_t	propulsive velocity increment applied at apoapsis of parking ellipse for apo-twist maneuver, miles/sec
$\Delta V_{2,a}$	propulsive velocity increment to transfer from ellipse apoapsis to circle of same radius, miles/sec
$\Delta V_{3,a}$	propulsive velocity increment to transfer from circle to ellipse with apoapsis equal to circular radius, miles/sec
$\sum \Delta V$	$\Delta V_1 + \Delta V_2 + \Delta V_3 + \Delta V_4$ for all-propulsive maneuvers; $\Delta V_1 + \Delta V_2 + \Delta V_3$ for full atmospheric braking at Earth return
X, Y	axes
x_∞, y_∞	coordinates of intersection of trajectory with Jupiter sphere of influence (see fig. 7)
α_H	path angle of interplanetary trajectory with respect to local horizontal, deg
α_∞	path angle of hyperbolic excess velocity with respect to local horizontal, deg
β	angle by which the hyperbolic excess velocity is turned by propulsion, deg (see fig. 12)

γ	angle between line of apsides of parking ellipse and direction of arrival hyperbolic excess velocity vector, deg
δ_i	turning due to planet gravity, from sphere of influence to periplanet, deg
ϵ	angle defining position of hyperbolic excess velocity on sphere of influence, deg (see fig. 7(b))
η_e	true anomaly on parking ellipse where spacecraft injects into parking orbit, deg
η_∞	true anomaly of sphere of influence on planetocentric hyperbolic trajectory, deg
θ	turning angle required between arrival and departure hyperbolic excess velocity vectors to perform a round trip, deg
λ	angle of rotation of parking orbit plane about line of apsides of parking ellipse, deg
μ	planet force constant, $miles^3/sec^2$
σ	turning angle to be supplied by parking orbit maneuver, deg
ψ	heliocentric angle, deg
ω	mean angular velocity of planet, deg/day

Subscripts:

a	apoapsis of elliptic parking orbit
b	homebound leg, from Jupiter periapsis to Earth periapsis
c	circular parking orbit
c1.1	circular parking orbit at 1.1 Jupiter radii
e	of elliptic trajectory
H	heliocentric
h	of hyperbolic trajectory
i	general subscript indicating either 2 or 3
o	outbound leg, from Earth periapsis to Jupiter periapsis
opt	optimum
p	periapsis
s	stay at Jupiter, from arrival to departure periapsis
T	total mission
t	apo-twist parking orbit
1	Earth departure
2	Jupiter arrival
3	Jupiter departure
4	Earth arrival
$\oplus$	Earth
$\mathfrak{4}$	Jupiter
∞	from sphere of influence to periplanet, or at sphere of influence

REFERENCES

1. Knip, Gerald, Jr.; and Zola, Charles L.: Three-Dimensional Sphere-of-Influence Analysis of Interplanetary Trajectories to Mars. NASA TN D-1199, 1962.

2. Knip, Gerald, Jr.; and Zola, Charles L.: Three-Dimensional Trajectory Analysis for Round-Trip Missions to Mars. NASA TN D-1316, 1962.

3. Zola, Charles L.; and Knip, Gerald, Jr.: Three-Dimensional Trajectory Analysis for Round-Trip Missions to Venus. NASA TN D-1319, 1962.

4. Clarke, V. C., Jr.; Roth, R. Y.; Bollman, W. E.; Hamilton, T. W.; and Pfeiffer, C. G.: Earth-Venus Trajectories, 1968-69. Rept. No. JPL-TM-33-99, Vol. 4, Pt. A, Jet Prop. Lab., C.I.T. (NASA CR-52465), Aug. 1, 1963.

5. Clarke, V. C., Jr.; Roth, R. Y.; Bollman, W. E.; Hamilton, T. W.; and Pfeiffer, C. G.: Earth-Venus Trajectories, 1970. Rept. No. JPL-TM-33-99, Vol. 5, Pt. B, Jet Prop. Lab., C.I.T. (NASA CR-53050), Oct. 1, 1963.

6. Luidens, Roger W.; and Kappraff, Jay M.: Mars Nonstop Round-Trip Trajectories. NASA TN D-2605, 1965.

7. Luidens, R. W.; and Miller, B. A.: Efficient Planetary Parking Orbits with Examples for Mars. NASA TN D-3220, 1966.

8. Planetary Flight Handbook. Vol. 3, pts. 1-3 of Space Flight Handbooks. NASA SP-35, pts. 1-3, 1963.

9. Ross, Stanley, ed.: Trajectories to Jupiter, Ceres, and Vesta. Planetary Flight Handbook, vol. 3, pt. 5 of Space Flight Handbook. NASA SP-35, pt. 5, 1966.

10. Gobetz, Frank W.: Optimum Transfers Between Hyperbolic Asymptotes. AIAA J., vol. 1, no. 9, Sept. 1963, pp. 2034-2041.

"The aeronautical and space activities of the United States shall be conducted so as to contribute . . . to the expansion of human knowledge of phenomena in the atmosphere and space. The Administration shall provide for the widest practicable and appropriate dissemination of information concerning its activities and the results thereof."

—NATIONAL AERONAUTICS AND SPACE ACT OF 1958

NASA SCIENTIFIC AND TECHNICAL PUBLICATIONS

TECHNICAL REPORTS: Scientific and technical information considered important, complete, and a lasting contribution to existing knowledge.

TECHNICAL NOTES: Information less broad in scope but nevertheless of importance as a contribution to existing knowledge.

TECHNICAL MEMORANDUMS: Information receiving limited distribution because of preliminary data, security classification, or other reasons.

CONTRACTOR REPORTS: Technical information generated in connection with a NASA contract or grant and released under NASA auspices.

TECHNICAL TRANSLATIONS: Information published in a foreign language considered to merit NASA distribution in English.

TECHNICAL REPRINTS: Information derived from NASA activities and initially published in the form of journal articles.

SPECIAL PUBLICATIONS: Information derived from or of value to NASA activities but not necessarily reporting the results of individual NASA-programmed scientific efforts. Publications include conference proceedings, monographs, data compilations, handbooks, sourcebooks, and special bibliographies.

Details on the availability of these publications may be obtained from:

SCIENTIFIC AND TECHNICAL INFORMATION DIVISION

NATIONAL AERONAUTICS AND SPACE ADMINISTRATION

Washington, D.C. 20546